MODEL REFERENCE ADAPTIVE SYSTEM BASED SPEED CONTROL OF SENSOR-LESS FIVE PHASE INDUCTION MOTOR

M.SC. THESIS

MELAKU TESFAYE SHIFERAW

HAWASSA UNIVERSITY, HAWASSA, ETHIOPIA

AUGUST, 2020

MODEL REFERNCE ADAPTIVE SYSTEM BASED SPEED CONTROL OF SENSOR-LESS FIVE PHASE INDUCTION MOTOR

MELAKU TESFAYE SHIFERAW

A THESIS SUBMITTED THE

DEPARTMENT OF ELECTRICAL AND COMPUTER ENGINEERING

HAWASSA INSTITUTE OF TECHNOLOGY,

SCHOOL OF GRATUATE STUDIES

HAWASSA UNIVERSITY

HAWASSA ETHIOPIA

IN PARTIAL FULFILMENT OF THE

REQUIRMENTS FOR THE DEGREE OF

MASTER OF SCINCE IN ELECTRICAL AND COMPUTER ENGINEERING

(CONTROL AND INSTRUMENTATION ENGINEERING)

JUNE,2020

SCHOOL OF GRADUATE STUDIES

HAWASSA UNIVERSITY

EXAMINERS' APPROVAL SHEET

We, the undersigned, members of the Board of Examiners the final open defense by **Mr. Melaku Tesfaye** Id.No. **PGCon/030/09**, have read and evaluate his thesis entitled **"Model Reference Adaptive System Based Speed Control of Sensor-less Five Phase Induction Motor",** and examined the candidate. This is, therefore to certify that the thesis has been accepted in partial fulfillment of the requirements for the degree.

Name of Chair Person	Signature	Date
Mr. Dereje Shibeshi		
Name of Major Advisor	Signature	Date
Name of Internal Examiner	Signature	Date
Name of External Examiner	Signature	Date
SGS Approval	Signature	Date

Declaration

I hereby declare that this MSc thesis entitled **"Model Reference Adaptive System Based Speed Control of Sensor-less Five Phase Induction Motor",** is my original work and has not been presented for a degree in any other university, and will not be presented by me to any other university for similar or any other degree award, and all source of material used for this thesis have been duly acknowledged.

Name: Melaku Tesfaye

Signature: _____

The MSc thesis entitled **"Model Reference Adaptive System Based Speed Control of Sensor-less Five Phase Induction Motor",** has been submitted for examination with my approval as thesis advisor.

Name: Mr. Dereje Shibeshi

Signature: _____

Place and date of submission: _____

Acknowledgements

Next to the Almighty God, I would like to articulate my deep gratitude and sincere thanks to my adviser Mr. Dereje Shibeshi for his most valuable guidance, critical comments and persistent encouragement.

Besides, I am thankful to my friend Workagegn Tatek for his timely help.

Last but not least, I would like to thank my precious parents for their great support and love during my study.

Abstract

This paper presents, rotor flux based model reference adaptive system speed estimator used for closed loop speed control of five phase induction motor without mechanical speed sensor. Multiphase motor drives with phase number greater than three phase leads to an improvement in the medium to high power drives application. The multiphase induction motor find application in special and critical area where high reliability is demanded such as Electric vehicles, aerospace application, ship propulsion and locomotive traction and in high power application. In principle, control methods for multi-phase machines are the same as for three-phase machines. Variable speed induction motor drives without mechanical speed sensors at the motor shaft have the attractions of low cost and high reliability. To replace the speed sensor, information of the rotor speed is extracted from measured stator currents and voltages at motor terminals. Vector-controlled drives require estimating the magnitude and spatial orientation of the fundamental magnetic flux in the stator or in the rotor. In this thesis, rotor flux based model reference adaptive system speed estimator is used for closed loop speed control of five phase induction motor without mechanical speed sensor with hysteresis current control. Model reference adaptive system designed to correct parameter variation to estimate the motor speed. As result the induction motor sensor-less control can operate over a wide range including zero speed. The sensor-less vector control operation has been verified by simulation on MATLAB. FOPI and PI controller was used for speed controller. The performance of two controllers has been verified through simulation results. It is seen that execute of the induction motor has improved when FOPI controller is used in place of classical PI controller.

Key words: Multi-phase, Five phase induction motor, MRAS, Current control, MATLAB, Sensor-less, FOPI

Table of Contents

List of Tables

List of Figures

List of Abbreviation

FOC	Field oriented control
MRAS	Model reference adaptive system
DC	Direct current
AC	Alternating current
PI	Proportional controller integral
IM	Induction motor
IFOC	Indirect field oriented control
DFOC	Direct field oriented control
HCC	Hysteresis current control
SVPWM	Space vector pulse width modulation
Back-emf	Back electromagnetic force
I_{qs-ref}	q-axis synchronous current Reference
I_{ds-ref}	d-axis synchronous current reference
I_{qs}	q-axis synchronous current
I_{ds}	d-axis synchronous current
$\widehat{\varphi}_r$	Estimated rotor flux
$\widehat{\omega_r}$	Estimated rotor speed
$\widehat{i_{ds}}$	Estimated stationary d stator current
$\widehat{i_{qs}}$	Estimated stationary q stator current
$\widehat{\varphi}_{dr}$	Estimated d axis rotor flux
$\widehat{\varphi}_{qr}$	Estimated q axis rotor flux

ω_e	Synchronous speed
ω_{sl}	Sleep speed
Lm	Mutual inductance
θ	Rotor flux angle
T_e	Electromagnetic torque
J	Moment of inertia
F	Frictional coefficient
T_L	Load torque
P	Pole pairs
K_P	Proportional gain
K_I	Integral gain
V_{dc}	DC link voltage

Subscripts

α -β	Relates to alpha and beta axis
d-q	Relates to direct and quadrature axis
1-3	Relates to first and third harmonics
S	Associated with stator winding
R	Associated with rotor winding
L	Associated with leakage

Chapter One

Introduction

1.1 Background of the study

The history of multiphase motor drive, known to the authors, dates to 1960, when five voltage source inverter-fed induction motor drive was proposed [1]. During the next 20 years' multiphase motor drives have attracted a steady but a rather limited attention. The pace started accelerating during the 1990s, but it was not until the beginning of this century that the multiphase motor drive has become a focus of a substantial worldwide attention with in the drives research community. This has predominantly resulted from developments in three very specific application areas, namely electric ship propulsion, traction and concept of more electric aircraft. Although the specific reasons for looking at a multiphase motor drive utilization in these application areas vary to a large extent, the common future is that utilization of multiphase motor drives is perceived as offering important advantage when compared to the use of their three phase counterpart.

In the recent time, Multi-Phase induction motors such as: five-phase, six phase, seven phase motor and so on, are fast increasing due to their several inherent benefits such as lower torque pulsation, reduction in harmonic currents, reduced stator current per phase without the need to increase the phase voltage, greater reliability, fault tolerant feature and increased power in the same frame as compared to three phase induction motor [2]. Presently the grid power available is only limited to three-phase so the supply to multi-phase motors is invariably given from power electronic converters.

Higher torque density in a multi-phase machine is possible, since apart from the fundamental spatial field harmonic, the space harmonic fields can be used to contribute to the total torque production. In a multi-phase machine, with five or more phases, there are additional degrees of freedom, which can be used to enhance the torque production through the injection of higher order current harmonics. The five-phase voltage source inverter inputs are decoupled into the torque producing (fundamental component) and third harmonics sets. This third harmonic current injection can be used to enhance the overall torque production [3].

Induction machines were chosen for variable speed drives, due to primarily low material and manufacturing cost and also reliable, associated with the squirrel cage induction machine is

proposed by [4]. In [5] were proposed accurate speed identification is required for all high performance vectors controlled induction motor drives. The speed identification of IM can be performed by a shaft speed encoder. However, compared to speed estimation, shaft speed encoder has several disadvantages such as an increase in cost, size, complexity, maintenance requirements and a decrease in the reliability and robustness. Speed encoders are expensive and introduce reliability concerns for vector controlled AC motor drives. The use of this encoder implies additional electronics, extra wiring, space and careful mounting which detracts from the inherent robustness of cage induction motors been proposed in [6]. Moreover, at low powers the cost of the sensor is about the same as the motor. Therefore, it has been great interest in the research community in developing a high performance induction motor drive that does not require a speed or position encoder for its operation. The concept of sensor-les vector control has been used for estimation techniques to estimate the speed of the rotor from motor terminal voltage and current signals. For high performance drives, vector control based systems can be used. These methods include rotor field orientation, feed forward control of stator voltages, stator flux orientation, estimation of rotor flux, torque current model, model reference adaptive system etc. Adaptive approaches are useful when machine parameters are not fully known. In this thesis the rotor speed estimation method for five phase induction motor has been done by rotor flux based model reference adaptive system. In the rotor flux based MRAS speed estimator the desired performance has been given in terms of a reference model and adaptive model. Each time an error is generated by comparing the reference and adaptive output. By considering this error, using suitable algorithm the gain expressions of the adaptive controller will be obtained. The MRAS speed estimator has been designed and test through various software tools. In this thesis design an adaptive estimator using the MATLAB simulation.

1.2 Statement of the problem

The trend of using multi-phase induction motor is obviously growing among the domestic and industrial application due to its characteristics. Multiphase motor drives with phase number greater than three phase leads to an improvement in the medium to high power drives application. The multiphase induction motor find application in special and critical area where high reliability is demanded such as Electric vehicles, aerospace application, ship propulsion and locomotive traction and in high power application. However, the drawback of having nonlinear characteristic make it difficult to be controlled. High performance vector controlled induction motor drives

require speed or position information for its operation. Generally, speed or position transducers provide this information. However, these mechanical sensors are costly and fragile. On the other hand, sensor-less drives operating without speed or position transducers have the advantage of reduced hardware complexity and lower cost, reduced size of the drive machine, elimination of the sensor cable, better noise immunity, increased reliability, and less maintenance requirements. To apply sensor-les induction motor estimation technique is required. The rotor speed of sensor-less induction motor can be estimated by different techniques. The rotor flux vector and slip calculation method are quite popular and simple to implement, but the accuracy is not very good. Other method is based on extended Kalman filter which is more robust to the induction motor parameter changes or identification errors but much more complicated in practical realization.

The solution for rotor speed estimation is based on MRAS principle, in which an error vector is formed from the outputs of reference and adaptive models, models both dependent on different motor parameters. The error is driven to zero through adjustment of the parameter that influences one of the models. The MRAS approach has advantages like simplicity and easy to implement which compared to other estimation schemes. Therefore, model reference adaptive system solves the problem due to aging, un-model dynamics and parameter variation even at low speed and are preferred and find applications in many areas for speed regulation.

1.3 Objectives

1.3.1 General objectives

To design Model Reference Adaptive system based Speed controller for sensor-les five phase induction motor using hysteresis current control pulse width modulation.

1.3.2 Specific objectives

- Modeling and study the characteristics of five phase induction motor
- Modeling of five phase induction motor vector control drive system
- Develop sensor-less speed estimation using model reference adaptive system
- Design and comparison of FOPI and conventional PI speed controller
- Simulating the speed control of five phase induction motor using vector control realized by hysteresis current control pulse width modulation
- Implement the whole integrated system using MATLAB/SIMULINK

1.4 Methodology

In this thesis work, indirect field oriented control based on the close loop rotor flux based MRAS speed estimator is used for the sensor-less speed control of five phase induction motor.

Due to effect of parameters variation on sensor-less speed control of five phase induction motor the reference and adaptive model is design properly. The reference model is used the induction motor itself and the adaptive model is the flux estimator models. The overall system includes two control loops, an inner current loop and an outer speed loop. Whenever a reference speed ω_r* , is given, the system automatically compares it with the motor actual speed ω_r, the speed error $\Delta\omega$, directly effects the torque profile. Therefore, the output of speed FOPI/PI regulator can be considered as the torque reference value. Correspondingly, the torque component iqs of the stator currents can be obtained. These measured currents are fed into the Clarke transformation block. The outputs of this projection are entitled $i_{s\alpha}$ and $i_{s\beta}$. These two components of the current enter into the Park transformation block that provide the current in the d, q reference frame.

The i_{sd} and i_{sq} components are contrasted to the references i_{sdref} (the flux reference) and i_{sqref} (the torque reference). At this instant, the control structure has an advantage to control induction machines by simply changing the flux reference and tracking rotor flux position. As induction motors need a rotor flux creation in order to operate, the flux reference must not be equal to zero. This easily eliminates one of the major shortcomings of the classic control structures the portability from asynchronous to synchronous drives. They are applied to the inverse Park transformation block. The outputs of this projection and measured currents are fed to the hysteresis current control pulse width modulation (HCCPWM) algorithm block. The outputs of this block provide signals that drive the inverter. Here both Park and inverse Park transformations need the rotor flux position. Finally, brief analysis depending on MATLAB simulation result will be given and checking of responses to different speed references with and without load disturbances, and parameter variation is going to be done. The General block diagram of this thesis work can be depicted in Figure. 1.1. Shown below.

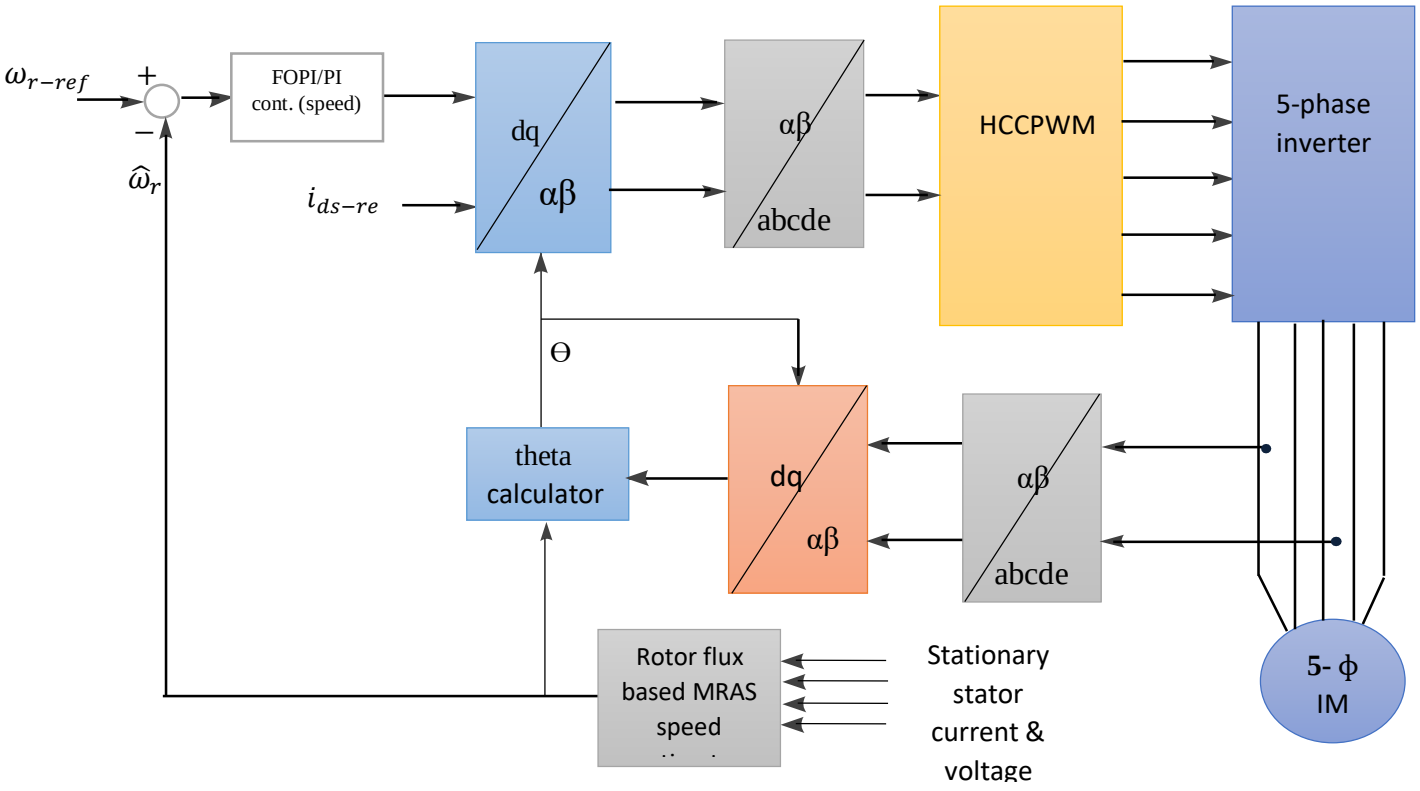

Figure 1.1 General block diagram of MRAS based sensor-less speed control of five phase induction motor

1.5 Thesis Organization

The thesis is organized including this introduction into six chapters including this introduction. The rest of the thesis is organized as follows.

Chapter 2 in this chapter discussed different literatures about control of multiphase and three phase induction motor.

Chapter 3 describes the theory and operation principle of five phase induction motor. Dynamical modeling of five phase induction motor with indirect field oriented vector control based on coordinate transformation fundamental and third harmonics components is described and sensor-less vector control and its principle is presented. The speed and the current control are designed based on the robust speed analysis. Furthermore, the dynamic model of five phase induction motor along with hysteresis current control pulse width modulation (HCC-PWM) and FOPI/PI speed controller are presented and are discussed.

Chapter 4 in this chapter sensor-less speed estimation of Five phase induction motor drive with indirect field oriented control based on rotor flux based model reference adaptive system is described. The details model and design of PI for MRAS based Speed estimator is presented.

Chapter 5 this chapter discussed on simulation of the drive system on MATLAB/Simulink including simulation result. Included in this chapter, simulation results based on load torque disturbance and motor parameter variation is discussed.

Chapter 6 this chapter summarizes the thesis and recommend further research possible in this area.

Chapter Two

Literature Review

Many prior research papers have been read about control of multiphase and three phase induction motors. Multi-phase machine and drives is a topic of growing relevance in recent years, and it presents many challenging issues that still need further research and it is becoming more and more a competitive system in many high performance drive applications, such as textile industry, paper mills, robotics and railway traction, require multi-phase electric drive. There are three main major components in an induction motor drive system: an induction motor, a power electronic device and a controller. The field orientation control, integrating modern control theory, power electronic and DSP/micro-processor technology, has made possible the development of high performance induction motor drive systems. The state of art of speed control of sensor-less induction motor and loss minimization is reviewed.

AC drives based on full digital control have reached the status of a mature technology. Ongoing research has concentrated on the elimination of the speed sensor at the machine shaft without deteriorating the dynamic performance of the drive control system. Problems associated with sensor less control systems have mainly included parameter sensitivity, integrator drift, and problems at low frequencies. Some have tried to solve these problems by redesigning the induction machine [7]. In [8] addressed a performance comparison between a three phase and a five phase inductions machine with the same rating and size. The analytical model considered saturation and losses. The cases analyzed showed that when all losses are accounted a better performance of five phase machines can be obtained when the machine design considers not only the air gap induction but also the overall losses. The comparison also demonstrated that an optimized trapezoidal air gap induction has a poorer performance in terms of efficiency and power factor, given that the joule and magnetic losses increase due the presence of the third harmonic induction. Reducing the harmonic content and choosing an optimal winding pitch allows to maximize the efficiency, leading to a better balance between additional losses and torque enhancement. It must be stressed that the five phase prototype machine analyzed has less stator and rotor winding volume as the three phase prototype machine, which has to be weighed against the reduced efficiency of the five phase machine in two of the three cases analyzed.

Martin Jones, Emil Levi, Slobodan N. Vukosavic have evaluated the feasibility and applicability of a parallel-connected five-phase two-motor drive. Dynamic and steady state models are presented and it is shown that the five-phase parallel-connected two-motor drive yields the same quality of dynamic operation, with full control decoupling between the machines in the group, as its series-connected counterpart. The parallel-connected five-phase drive retains all the benefits of the series connection, such as the saving in the number of inverter legs, the ability to control two machines using only one DSP, and the possibility of direct utilization of the braking energy as well as the additional benefit of using standard star connected windings. However, compared to an equivalent series-connected system, the parallel configuration suffers from a number of serious shortcomings. It is believed that these shortcomings will prevent its application in the form investigated here in industry [9].

A. Iqbal & E. Levi have analyzed different space vector PWM (SVM) schemes for a five phase voltage source inverter, which can be used for five-phase motor drives. It is shown that the standard method, based on utilization of large vector only, produces output phase voltages with a substantial low order harmonic content. A new SVM techniques using both large and medium vectors are therefore devised, with the idea of achieving an output voltage waveform as close as possible to sinusoidal, while simultaneously keeping the switching frequency constant and enabling full utilization of the available DC bus voltage. The new technique is elaborated in literature in details [10]. Tze-Fun Chan and Keh Shi have discussed the indigent control of induction motor drives. The performance of the controller used in drives should be independent of, or less sensitive to, motor parameter changes. Base on theories of induction motor and control principle, expert-system control, fuzzy-logic control, neural network control and genetic algorithm of induction motor drive have investigated and developed. Artificial neural network has been developed in literature and implemented with five-phase induction motor to achieve insensitive operation [11].

E. Levi, R. Bojoi, F Profume, H.A. Toliyat have been presented state of-the-art and highlight recent developments in the area of multi-phase induction motor drive. Advantages and applications of multi-phase induction motor have discussed in details. It was shown that additional degrees of freedom in multi-phase machines can be employed to improve the overall performance of the system. They are being used to improve the reliability of a multiphase system, to enhance the torque production capability of the machine by injecting harmonics of current or to control multi-

motors from a single inverter [10]. Bifurcation Analysis of Five-Phase Induction Motor Drives with Third Harmonic Injection was developed in [12]. This paper addresses, for the first time, the bifurcation analysis of a five-phase induction motor drive when a third harmonic is injected for torque enhancement purposes. The main focus of the paper is to present a mathematically based study of the nonlinear dynamics of the proposed drive with torque enhancement. The overall bifurcation analysis for both concentrated and distributed winding machines, that the harmonic injection provides not only torque enhancement but also more robust controllers.

An application of rotor field oriented control to a five-phase induction motor with the combined fundamental and third harmonic currents was proposed in [13]. In the proposed technique the complete theory and modeling of RFOC of the five-phase induction motor are established. Specifically, investigation is made to improve power density and output torque of the five-phase induction motor by injecting third harmonic of currents. By the proper dynamical adjustment and steady state compensation, the rotor field oriented control of the five-phase induction motor not only achieves a high drive performance, but also controls the fundamental and third harmonic flux and torque to generate the desired nearly rectangular air-gap flux.

Five-Phase Induction Motor Drives with DSP-Based Control System was proposed in [14]. This introduces two kinds of control schemes: vector control and direct torque control. The implementation of these control systems was done using 32-bit floating point TMS320C32 DSP. Vector control of the five-phase induction motor not only achieves high drive performance, but also generates the desired nearly rectangular current waveforms and flux profile in the air-gap resulting in an improvement in air gap flux density and an increase of 10% in output torque. Among different model-based types of speed estimation system configurations, MRAS is important because it results to relatively easy to implement with high speed adaptation for a wide range of applications. The high performance ability and easy stability analysis of the MRAS make it as one of the major approaches in adaptive control. The advantage of MRAS is to allow an improved noise rejection property which is helpful to obtain unbiased parameter estimation. Rotor flux MRAS, principally developed by C. Schauder [15], is the most established MRAS strategy and much effort has aimed at improving its performance

.

Chapter Three

Modeling and Field Oriented Control of Five Phase Induction Motor

3.1 Introduction

For control induction motor drive numerous control strategies are employed having good steady state response but poor dynamic response due to the deviation of air gap flux linkage from its set value. This deviation is not only in magnitude but also in phase. This deviation of the linkage flux can be controlled by the magnitude and frequency of the rotor and the stator current and their instantaneous phases. This chapter presents field oriented control of five phase induction motor based on mathematical transformations of the standard five phase induction motor model into specific two phase d-q coordinate model. The five phase induction motor model is a complex matrix equation with sinusoidal functions of the rotor flux the rotor flux was proposed in [16]. This model has inherent control and computation disadvantages due to the ever changing rotor flux. This can be greatly improved with a simple transformation of the five phase model into a d-q model with the two coordinates rotate with respect to the rotor flux at the synchronous speed. The five phase stator current of the induction motor may be modeled as a complex space vector which can be transformed into two currents the d-coordinate stator current and the q-coordinate stator current. The d-coordinate stator current chosen to be in line with the d-axis rotor flux and the q-coordinate stator current chosen to be 90° lagging. This transformation also gives significant computational advantage in the field oriented control of induction motors.

In this chapter, the mathematical model of five phase induction motor based on space vector theory and the principle of indirect FOC are presented. The simulation model of the induction motor drive is developed using the principle of indirect FOC.

3.2 Induction Motor

An induction or asynchronous motor is an AC electric motor in which the electric current in the rotor needed to produce torque is obtained by electromagnetic induction from the magnetic field of the stator winding. Induction refers to the field in the rotor is induced by the stator current and asynchronous refers to the fact that the rotor speed is not equal to the stator speed. No

sliding contacts and permanent magnets are needed to make an induction motor work which makes it very simple and cheap to manufacture. As motors, they rugged and require very little maintenance. However, the speed is not as easily controlled as with DC motors and they draw large starting currents, and operate with a poor lagging factor when lightly loaded was proposed [17].

3.2.1 Construction of the five Phase Induction Motor

AC induction motors are commonly used in industry applications. This type of motor has three main parts; rotor, stator and enclosure. The stator and the rotor do the work and the enclosure protects the stator and rotor. Most induction motors are rotary type with basically a stationary stator and a rotating rotor. The stator has a cylindrical magnetic core that is housed inside a metal frame. The stator magnetic core is formed by stacking thin electrical steel laminations with uniformly spaced slots stamped in the inner circumference to accommodate the three distributed stator windings. The stator windings are formed by connecting coils of copper or aluminum conductors that are insulated from the slot walls. The rotor consists of a cylindrical laminated iron core with uniformly spaced peripheral slots to accommodate the rotor windings.

There are two different types of induction motor rotor; Wound rotor induction motor has a five phase winding, similar to the stator winding. The rotor winding terminals are connected to five slip rings which turn with the rotor. The slip rings/brushes allow external resistors to be connected in series with the winding. The external resistors are mainly used during start-up under normal running conditions the windings short circuited externally. The second type of induction motor rotor is the squirrel cage rotor. It consists of series of conducting bars laid into slots carved in the face of rotor and shorted at either end by large shorting rings. In this thesis a squirrel cage rotor induction motor is used.

3.2.2 Principle of Five Phase Induction Motor

Similar to the working of three phase induction motor, five phase induction motor works on the application of Faraday's law and Lorentz force on conductor. When five phase ac supply is given to the stator winding which are spatially and time displaced 72° the rotating magnetic field is produce which rotates at synchronous speed. When short circuited rotor (squirrel cage) is placed in rotating magnetic field an EMF is induced in the rotor conductor due to electromagnetic

induction. Due to this EMF, current starts flowing in the rotor conductor and sets up its own magnetic field. Due to interaction of these two magnetic fields, a torque is produced and conductor tends to move.

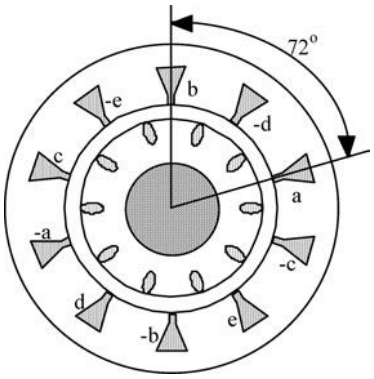

Figure 3.1 Five-phase concentrated-winding induction machine

3.2.3 Dynamic Model of Five Phase Induction Motor

A dynamic model of the five phase induction motor subjected to control must be known in order to understand and design the vector controlled drives and speed estimation technique. Such a model can be obtained by means of the two axis theory of electrical motors. Following are the assumptions made for the model:

- The five-phase motor is symmetrical, only the fundamental and the third harmonic is considered, while the higher harmonics of the spatial field distribution and of the magneto motive force (MMF) in the air gap are disregarded,
- The effects of anisotropy, magnetic saturation, iron losses and eddy currents are neglected,
- The coil resistances and reactance are taken to be constant,

In this thesis, a complex vector notation and some reference frame conversions are used. Since this is quite essential to the understanding of the rest of the theory, it was shortly described in the following subsection.

3.3 Five phase Transformation

In this thesis generalized machine theory and mathematical transformations are used to decouple variables to facilitate the solution of difficult equation with time varying coefficients or to refer all variables in a common reference frame. The most commonly used transformation is poly-phase to orthogonal two phase transformation. For the n-phase to two phase case, it can be expressed in the form of:

$$[f_{xy}]=[T_{(\theta)}][f_1, f_2, f_3 \dots n]^T \tag{3.1}$$

$$[T_{(\theta)}] = \sqrt{2/n}\begin{bmatrix} cos\frac{p}{2}\theta & \cos(\frac{p}{2}\theta-\alpha) & \dots \\ sin\frac{p}{2}\theta & \sin(\frac{p}{2}\theta-\alpha) & \dots \end{bmatrix} \tag{3.2}$$

Where , α is the electrical angle between the two adjacent magnetic axes of a uniformly distributed n-phase winding ;The coefficient $\sqrt{2/n}$ is introduced to make the transformation power invariant .Important subset of the general n-phase to two phase transformation ,though not necessarily power invariant ,these are discussed in the following section.

3.3.1 The Clarke and Parke Transformation

The Clarke and Parke transformation is a transformation of coordinates that designed to transform multi-phase stationary coordinate system in to two axes stationary and rotating coordinate system respectively. Clarke transform uses five-phase voltages these two voltages in the fixed coordinate stator phase are transformed to the $v_a, v_b, v_c, v_d \; and \; v_e$.

To calculate voltages in the two-phase orthogonal stator axis , $v_\alpha \; and \; v_\beta$.These two voltages in the fixed coordinate stator phase are transformed to the $v_d \; and \; v_q$voltage components in the dq frame with the Park transform. Park transformation is used to transform from the stationary reference frame $(\alpha - \beta)$ in to the rotating reference frame (d-q).

Considering squirrel-cage induction motor, the transformations are usually based on the following assumptions:

- Slot harmonics and deep bar effects are not considered.
- Space harmonics of the flux linkage distribution are neglected.
- Iron losses are not taken into account.
- Saturation is neglected.
- Neutral point is isolated

The transformation of five-phase induction motor variables can be made in two steps; these are:

i. Five-phase to two phase transformation
ii. Two phase stationary to two phase synchronously rotating frame transformation

3.3.2 Five- phase to Two Phase Transformation

A transformation from the five-phase stationary coordinate system to the two-phase $(\alpha - \beta)$ stationary coordinate system is called Clarke Transformation. This transformation block is responsible for translating five axes to two axes system reference to the stator. Two of the five phase currents are measured because the sum of the five phase currents equal to zero. Basically the transformation shifts from a five axis, two- dimensional coordinate system attached to the stator of the motor to a two axis system referred to the stator. The measured current represents the vector component of the current in a five axis coordinate system which are spatially separated by 72°. Clarke transformation transforms the rotating current vector in a two axis orthogonal coordinate system, so that the current vector is represented with two vector components which vary with time. The space vector can be transformed to another reference frame with only two orthogonal axis called α β, where the axis 'α' and axis 'a' coincide each other. Figure 3.2 shows the stator current space vector and its component in stationary reference frame and the Clarke transformation module.

The idea of Clarke transformation is that the rotating stator current vector that is the sum of the five-phase currents can also be generated by a bi-phased system placed on the fixed axis $\alpha \; and \; \beta$.In symmetrical five-phase machines with stationary v_{as}-v_{bs}-v_{cs}-v_{ds}-v_{es} axes at 72 degree apart, the alpha and beta axis stator voltages $v_{\alpha} and \; v_{\beta}$ are fictitious quadrature phase (two-phase) voltage components, which are related to the actual five-phase stator voltages as follows [18]:

$$
\begin{aligned}
v_{\alpha 1} &= k(v_a + v_b \cos\left(\frac{2\pi}{5}\right) + v_c * \cos\left(\frac{4\pi}{5}\right) + v_d * cos\left(\frac{4\pi}{5}\right) + v_e * \cos\left(\frac{2\pi}{5}\right)) \\
v_{\beta 1} &= k(0 + v_b \sin\left(\frac{2\pi}{5}\right) + v_c * \sin\left(\frac{4\pi}{5}\right) - v_d * \sin\left(\frac{4\pi}{5}\right) - v_e \sin\left(\frac{2\pi}{5}\right)) \qquad (3.3) \\
v_{\alpha 3} &= k(v_a + v_b \cos\left(\frac{6\pi}{5}\right) + v_c * \cos\left(\frac{2\pi}{5}\right) + v_d * \cos\left(\frac{2\pi}{5}\right) + v_e \cos\left(\frac{6\pi}{5}\right)) \\
v_{\beta 3} &= k(0 + v_b \sin\left(\frac{6\pi}{5}\right) + v_c * \sin\left(\frac{2\pi}{5}\right) - v_d * \sin\left(\frac{2\pi}{5}\right) - v_e * \sin\left(\frac{6\pi}{5}\right))
\end{aligned}
$$

In matrix form of the five-phase to two phase transformation of the stator voltage (a, b, c, d, e) to $(\alpha - \beta)$ is given as:

$$\begin{bmatrix} v_{\alpha 1} \\ v_{\beta 1} \\ v_{\alpha 3} \\ v_{\beta 3} \end{bmatrix} = \frac{2}{5} \begin{bmatrix} 1 & \cos\left(\frac{2\pi}{5}\right) & \cos\left(\frac{4\pi}{5}\right) & cos\left(\frac{4\pi}{5}\right) & \cos\left(\frac{4\pi}{5}\right) \\ 0 & \sin\left(\frac{2\pi}{5}\right) & \sin\left(\frac{4\pi}{5}\right) & -\sin\left(\frac{4\pi}{5}\right) & \sin\left(\frac{2\pi}{5}\right) \\ 1 & \cos\left(\frac{6\pi}{5}\right) & \cos\left(\frac{2\pi}{5}\right) & \cos\left(\frac{2\pi}{5}\right) & \cos\left(\frac{6\pi}{5}\right) \\ 0 & \sin\left(\frac{6\pi}{5}\right) & \sin\left(\frac{2\pi}{5}\right) & -\sin\left(\frac{2\pi}{5}\right) & \sin\left(\frac{6\pi}{5}\right) \end{bmatrix} \begin{bmatrix} v_a \\ v_b \\ v_c \\ v_d \\ v_e \end{bmatrix} \quad (3.4)$$

Similarly, for stator current the matrix forms of a five phase to two phase transformation (a b c d and e) to $\alpha - \beta$ is also given as:

$$\begin{bmatrix} i_{\alpha 1} \\ i_{\beta 1} \\ i_{\alpha 3} \\ i_{\beta 3} \end{bmatrix} = \frac{2}{5} \begin{bmatrix} 1 & \cos\left(\frac{2\pi}{5}\right) & \cos\left(\frac{4\pi}{5}\right) & cos\left(\frac{4\pi}{5}\right) & \cos\left(\frac{4\pi}{5}\right) \\ 0 & \sin\left(\frac{2\pi}{5}\right) & \sin\left(\frac{4\pi}{5}\right) & -\sin\left(\frac{4\pi}{5}\right) & \sin\left(\frac{2\pi}{5}\right) \\ 1 & \cos\left(\frac{6\pi}{5}\right) & \cos\left(\frac{2\pi}{5}\right) & \cos\left(\frac{2\pi}{5}\right) & \cos\left(\frac{6\pi}{5}\right) \\ 0 & \sin\left(\frac{6\pi}{5}\right) & \sin\left(\frac{2\pi}{5}\right) & -\sin\left(\frac{2\pi}{5}\right) & \sin\left(\frac{6\pi}{5}\right) \end{bmatrix} \begin{bmatrix} i_a \\ i_b \\ i_c \\ i_d \\ i_e \end{bmatrix} \quad (3.5)$$

Equation 3.4 and 3.5 are valid only for balanced system otherwise zero sequence components are introduced. The simplified diagram of a five-phase induction motor in figure 3.2 shows the stator winding for each phase displaced $2\pi/5$ radians in space and their wave forms.

The transformation of stator variables to a two-phase reference frame (indicated by subscripts α-β), where the coils are perpendicular, guarantees that there is no interaction between perpendicular windings as long as there is no saturation.

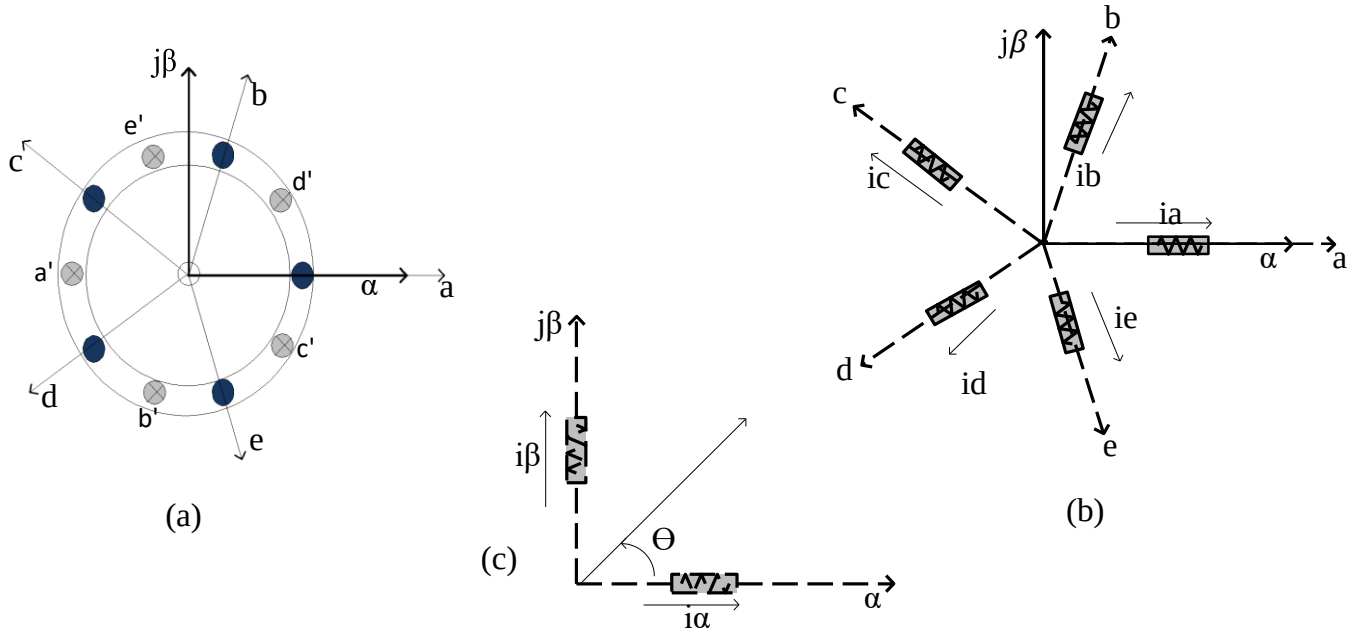

Figure 3.2 (a) five-phase windings, (b) five-phase reference frame wave form and (c) two-phase axes equivalent

3.3.3 Two Phase Stationary to Two Phase Synchronously Rotating Frame Transformation

A transformation from the $(\alpha - \beta)$ stationary coordinate system to the d-q rotating coordinate system is called Park Transformation. It is used to rotate the two axis coordinate system so that it is aligned with the rotating motor and this projection modifies a two phase orthogonal α-β system in the d-q rotating reference frame. The stator reference frame is not suitable for the control process. The space vector i_s is rotating at a rate equal to the angular frequency of the phase currents, the components change with time and speed. In order to gain a complete decoupling of torque and flux, the current phasor is transformed into two components of a rotating reference frame rotating at the same speed as the angular frequency of the phase currents, these components do not depend on time and speed. In FOC this is the most important transformation, the component of stator current which is responsible for the rotor flux can be fix to the d axis. These components depend on the α-β current vector components and the rotor flux position. The separate flux and the torque components of stator current vector in two coordinate time invariant system can be expressed by (2.6). Direct torque control is possible and becomes easy with the flux component i_{ds} aligned with the d axis representing the direction of the rotor flux and torque component i_{qs} aligned with the q axis perpendicular to the rotor flux. Figure 3.3 shows the stator current space vector and its component in rotating reference frame and the Park transformation module. The d-q reference frame is rotating at speed $\alpha - \beta$ axes as shown in figure 3.3. The angle between α and d axis $\theta_e = \omega_e t$.

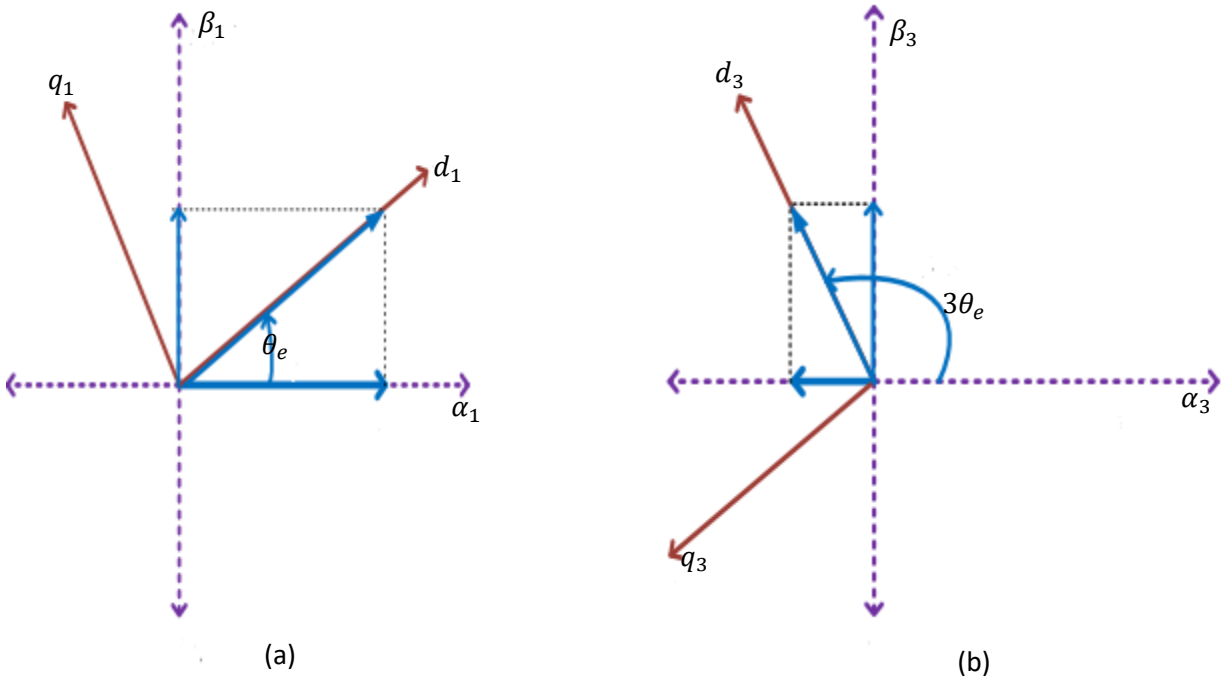

Figure 3.3 (a) d_1-q_1 reference frame, (b) d_3-q_3 reference frame

The voltage v_α ,v_β can be converted to voltages on d-q axis according to the following relations:

$$\begin{aligned} v_{d1} &= v_{\alpha1} * \cos(\theta_e) + v_{\beta1} * \sin(\theta_e) \\ v_{q1} &= -v_{\alpha1} * \sin(\theta_e) + v_{\beta1} * \cos(\theta_e) \\ v_{d3} &= v_{\alpha3} * \cos(3\theta_e) + v_{\beta3} * \sin(3\theta_e) \\ v_{q3} &= -v_{\alpha3} * \cos(3\theta_e) + v_{\beta3} * \cos(3\theta_e) \end{aligned} \tag{3.6}$$

In matrix form of the two phase stationary to two phase synchronously rotating frame transformation is given as:

$$\begin{bmatrix} v_{d1} \\ v_{q1} \\ v_{d3} \\ v_{q3} \end{bmatrix} = \frac{2}{5} \begin{bmatrix} \cos(\theta_e) & \sin(\theta_e) & 0 & 0 \\ -\sin(\theta_e) & \cos(\theta_e) & 0 & 0 \\ 0 & 0 & \cos(3\theta_e) & \sin(3\theta_e) \\ 0 & 0 & -\sin(3\theta_e) & \cos(3\theta_e) \end{bmatrix} \begin{bmatrix} v_{\alpha1} \\ v_{\beta1} \\ v_{\alpha3} \\ v_{\beta3} \end{bmatrix} \tag{3.7}$$

3.3.4. Inverse Park Transformation

In this transformation, the stator voltages represented in the d-q rotating reference frame are transformed to a two phase orthogonal α-β system, from which we can obtain the reference vector components to be applied to the motor phases.

The projection that modifies the d-q rotating reference frame to two phase orthogonal system is expressed by (3.8).

In the reverse way; the transformation of rotating frame parameters to stationary frame is given according to the following relations:

$$\begin{aligned} v_{\alpha 1} &= v_{d1} * \cos(\theta_e) - v_{q1} * \sin(\theta_e) \\ v_{\beta 1} &= v_{d1} * \sin(\theta_e) + v_{q1} * \cos(\theta_e) \\ v_{\alpha 3} &= v_{d3} * \cos(3\theta_e) - v_{q3} * \sin(3\theta_e) \\ v_{\beta 3} &= v_{d3} * \sin(3\theta_e) + v_{q3} * \cos(3\theta_e) \end{aligned} \tag{3.8}$$

In matrix form representation is given as:

$$\begin{bmatrix} v_{\alpha 1} \\ v_{\beta 1} \\ v_{\alpha 3} \\ v_{\beta 3} \end{bmatrix} = \frac{2}{5} \begin{bmatrix} \cos(\theta_e) & -\sin(\theta_e) & 0 & 0 \\ \sin(\theta_e) & \cos(\theta_e) & 0 & 0 \\ 0 & 0 & \cos(3\theta_e) & -\sin(3\theta_e) \\ 0 & 0 & \sin(3\theta_e) & \cos(3\theta_e) \end{bmatrix} \begin{bmatrix} v_{d1} \\ v_{q1} \\ v_{d3} \\ v_{q3} \end{bmatrix} \tag{3.9}$$

The general Park transformation $v_d \; and \; v_q$ can be also obtained directly from v_a , v_b , v_c $v_d \; and \; v_e$ the matrix equation corresponding to this transformation is given as.

$$\begin{bmatrix} v_{d1} \\ v_{q1} \\ v_{d3} \\ v_{q3} \end{bmatrix} = \frac{2}{5} \begin{bmatrix} v_a \\ v_b \\ v_c \\ v_d \\ v_e \end{bmatrix} \begin{bmatrix} \cos(\theta_e) & \cos\left(\theta_e - \frac{2\pi}{5}\right) & \cos\left(\theta_e - \frac{4\pi}{5}\right) & cos\left(\theta_e - \frac{6\pi}{5}\right) & \cos\left(\theta_e - \frac{8\pi}{5}\right) \\ -\sin(\theta_e) & -\sin\left(\theta_e - \frac{4\pi}{5}\right) & -\sin\left(\theta_e - \frac{4\pi}{5}\right) & -\sin\left(\theta_e - \frac{6\pi}{5}\right) & -\sin\left(\theta_e - \frac{8\pi}{5}\right) \\ \cos(3\theta_e) & \cos\left(3(\theta_e - \frac{2\pi}{5})\right) & \cos\left(3(\theta_e - \frac{4\pi}{5})\right) & \cos\left(3(\theta_e - \frac{6\pi}{5}\right) & \cos\left(3(\theta_e - \frac{8\pi}{5})\right) \\ -\sin(3\theta_e) & -\sin\left(3(\theta_e - \frac{2\pi}{5})\right) & -\sin\left(3(\theta_e - \frac{6\pi}{5})\right) & -\sin\left(3(\theta_e - \frac{2\pi}{5})\right) & -\sin\left(3(\theta_e - \frac{8\pi}{5})\right) \end{bmatrix} \tag{3.10}$$

Since the actual stator variables either to be generated or to be measured are all in stationary a-b-c-d-e frame, synchronous frame transform should be executed in the control. The most popular transform between stationary a-b-c-d-e frame quantities to synchronously rotating d-q quantities is given in equation (3.10)

3.4 D-Q Dynamic Model of Induction Motor in the Synchronous Frame

The mathematical model of IM variables such as: stator voltage, rotor voltage, stator flux linkage and rotor flux linkage are represented in the synchronous reference frame [19].

The stator voltage equations:

$$v_{ds1} = R_S \, i_{ds1} + \frac{d}{dt}\varphi_{ds1} - \omega_e \varphi_{qs1} \tag{3.11}$$

$$v_{qs1} = R_S \, i_{qs1} + \frac{d}{dt}\varphi_{qs1} + \omega_e \varphi_{ds1} \tag{3.12}$$

$$v_{ds3} = R_S\, i_{ds3} + \frac{d}{dt}\varphi_{ds3} - 3\omega_e \varphi_{qs3} \quad (3.13)$$

$$v_{qs3} = R_S\, i_{qs3} + \frac{d}{dt}\varphi_{qs3} + 3\omega_e \varphi_{ds3} \quad (3.14)$$

The rotor voltage equations:

$$v_{dr1} = 0 = R_r * i_{dr1} + \frac{d}{dt}(\varphi_{dr1}) - (\omega_e - \omega_r)\varphi_{qr1} \quad (3.15)$$

$$v_{qr1} = 0 = R_r * i_{qr1} + \frac{d}{dt}(\varphi_{qr1}) + (\omega_e - \omega_r)\varphi_{dr1} \quad (3.16)$$

$$v_{dr3} = 0 = R_r * i_{dr3} + \frac{d}{dt}(\varphi_{dr3}) - 3(\omega_e - \omega_e)\varphi_{qr3} \quad (3.17)$$

$$v_{qr3} = 0 = R_r * i_{qr3} + \frac{d}{dt}(\varphi_{qr3}) + 3(\omega_e - \omega_r)\varphi_{dr3} \quad (3.18)$$

The stator flux linkage equation:

$$\varphi_{ds1} = L_S\, i_{ds1} + L_m\, i_{dr1} \quad (3.19)$$

$$\varphi_{qs1} = L_S\, i_{qs1} + L_m\, i_{qr1} \quad (3.20)$$

$$\varphi_{ds3} = L_S\, i_{ds3} + L_m\, i_{dr3} \quad (3.21)$$

$$\varphi_{qs3} = L_S\, i_{qs3} + L_m\, i_{qr3} \quad (3.22)$$

The rotor flux linkages equations:

$$\varphi_{dr1} = L_r\, i_{dr1} + L_m\, i_{ds1} \quad (3.23)$$

$$\varphi_{qr1} = L_r\, i_{qr1} + L_m\, i_{qs1} \quad (3.24)$$

$$\varphi_{dr3} = L_{lr}\, i_{dr3} + L_m\, i_{ds3} \quad (3.25)$$

$$\varphi_{qr3} = L_{lr}\, i_{qr3} + L_m\, i_{qs3} \quad (3.26)$$

Where φ_{ds} φ_{qs} : d-axis and q-axis stator flux linkage , φ_{dr} , φ_{qr} : d-axis and q-axis rotor flux linkages R_s , R_r : Stator and rotor resistance , v_{ds} , v_{qs} : d-axis and q- axis stator voltage , v_{dr} , v_{qr} : d-axis and q- axis rotor voltage , v_{dr} , v_{qr} : d-axis and q- axis rotor voltage , i_{ds} , i_{qs} : d -axis and q-axis stator current , i_{dr} , i_{qr} : d- axis and q-axis rotor current, ω_e, ω_r : Synchronous speed and rotor speed and L_S , L_{lr} , L_m : Stator self-inductance, rotor self -inductance and mutual inductance respectively.

The d-q space vector method is generally used to describe the model of the induction motor. The advantage of this method is as follows:

- Reduction of the number of dynamic equations,
- Possibility of analysis at any supply voltage waveform,
- The equations can be represented in various rectangular coordinate systems.

3.5 Field Oriented Control of Five Phase Induction Motor

The concept of field orientation control is used to accomplish a decoupled control of flux and torque. Field Oriented Control can be used to vary the speed of an induction motor over a wide range. It was initially developed by Blaschke in [20]. It is commonly known as vector control because it controls both the magnitude and phase of the variables. In the vector control scheme, a complex current is synthesized from two current components, one of which is responsible for the flux level in the motor and another which controls the torque production in the motor. Vector control offers a number of benefits including speed control over a wide range, precise speed regulation, fast dynamic response and operation above base speed by Mircea Popescu in [21]

3.6 Principles of Vector control

In FOC, the principle of decoupled torque and flux control are applied and it relies on the instantaneous control of stator current space vectors. Control of induction motor is complicated due to the control of decoupled torque and flux producing components of the stator phase currents. There is no direct access to the rotor quantities such as rotor fluxes and currents. To overcome these difficulties, high performance vector control algorithms are developed which can decouple the stator phase currents by using only the measured stator current, flux and rotor speed.

There are two approaches to obtain the flux vector, one direct measurement and other is indirect. According to the field oriented control can be classified as direct field orientation control (DFOC) and indirect field orientation control (IFOC).

3.6.1 Direct vector control

In case of direct vector control the motor flux is measure by directly measure the air gap fluxes using Hall Effect sensors by Bimal K.Bose in [22]. However, the drift in the integrator with a search coil is problematic at very low frequencies and it tends to be temperature sensitive and fragile. An alternative approach is to measure the terminal voltage and phase currents of the machine and use these to estimate the flux.

Direct vector controlled drive, the controlled depend on stator resistance. Therefore, for perfect decoupling of flux and torque, estimation and compensation for these parameter variations is necessary. Also for certain speed sensor-less drives, the estimation technique is depending on plant

parameters technique is dependent on plant parameters. In such cases, compensation for variation parameters is an absolute necessity [23]. Not only for control or estimation in drives, non-hostile methods of winding temperature estimation using stator resistance identification has been found to be very reliable. In the direct field oriented control the stator frequency of the drive is not controlled. The motor is self-controlled by using the unit vector to help control the frequency and phase. There is no concern about instability because limiting within the safe limit automatically limits operation to the stable region. Transient response will be fast because torque control by does not affect flux. Vector control allows for speed control in all four quadrants since negative torque is directly taken care of in vector control[24].

3.6.2. Indirect Field Oriented Control

In indirect field orientation, the synchronous speed we is the same as the instantaneous speed of the rotor flux vector and the d-axis of the d-q coordinate system is exactly locked on the rotor flux vector (rotor flux vector orientation).

Indirect field oriented control; here the rotor flux angle is being measured indirectly, Instead of using air gap flux sensors. IFOC estimates the rotor flux by computing the slip speed (ω_{sl}). The stationary d and q axes are fixed on the stator and the rotor d and q axes are fixed on the rotor flux. The synchronous d and q-axes are rotating at synchronous speed and so there is a slip difference between the rotor speed and the synchronous speed given by:

$$\theta_e = \int \omega_e \mathrm{dt} = \int (\omega_{sl} + \omega_r)\ \mathrm{dt} \tag{3.27}$$

In order to ensure decoupling between the rotor flux and the torque, the torque component of the current should be aligned with the synchronous q axis and the stator flux component of current should be aligned with the synchronous d-axis.

Equating Equation (3.11) to Equation (3.24) and rotor flux linkage equations, the rotor flux and stator current written as follows:

$$\frac{d}{dt} i_{ds1} = \frac{1}{\sigma L_S} v_{ds1} - \frac{1}{\sigma L_S}\left(R_S + \frac{L_m{}^2}{L_r T_r}\right) i_{ds1} + \omega_e i_{qs1} + \frac{1}{\sigma L_S}\frac{L_m}{T_r}\varphi_{dr1} + \frac{1}{\sigma L_S}\frac{L_m}{L_r}\omega_r \varphi_{qr1} \tag{3.28}$$

$$\frac{d}{dt} i_{qs1} = \frac{1}{\sigma L_S} v_{qs1} - \frac{1}{\sigma L_S}\left(R_S + \frac{L_m{}^2}{L_r T_r}\right) i_{qs1} - \omega_e i_{ds1} - \frac{1}{\sigma L_S}\frac{L_m}{T_r}\varphi_{dr1} + \frac{1}{\sigma L_S}\frac{L_m}{L_r T_r}\omega_r \varphi_{qr1} \tag{3.29}$$

$$\frac{d}{dt} i_{ds3} = \frac{1}{\sigma L_S} v_{ds3} - \frac{1}{\sigma L_S}\left(R_S + \frac{L_m{}^2}{L_r T_r}\right) i_{ds3} + 3\omega_e i_{qs3} + \frac{1}{\sigma L_S}\frac{L_m}{L_r T_r}\varphi_{dr3} + 3\frac{1}{\sigma L_S}\frac{L_m}{L_r}\omega_r \varphi_{qr3} \tag{3.30}$$

$$\frac{d}{dt}i_{qs3} = \frac{1}{\sigma L_S}v_{qs1} - \frac{1}{\sigma L_S}\left(R_S + \frac{L_m{}^2}{L_r T_r}\right) i_{qs3} - 3\omega_e i_{ds3} - 3\frac{1}{\sigma L_S}\frac{L_m}{L_r}\omega_r \varphi_{dr3} + \frac{1}{\sigma L_S}\frac{L_m}{L_r T_r}\varphi_{qr3} \quad (3.31)$$

$$\frac{d}{dt}\varphi_{dr1} = \frac{L_m}{T_r} i_{ds1} - \frac{1}{T_r}\varphi_{dr1} + (\omega_e - \omega_r)\varphi_{qr1} \quad (3.32)$$

$$\frac{d}{dt}\varphi_{qr1} = \frac{L_m}{T_r} i_{qs1} - (\omega_e - \omega_r)\varphi_{dr1} - \frac{1}{T_r}\varphi_{qr1} \quad (3.33)$$

$$\frac{d}{dt}\varphi_{dr3} = \frac{L_m}{T_r} i_{ds3} - \frac{1}{T_r}\varphi_{dr3} + 3(\omega_e - \omega_r)\varphi_{qr3} \quad (3.34)$$

$$\frac{d}{dt}\varphi_{qr3} = \frac{L_m}{T_r} i_{qs3} - 3(\omega_e - \omega_r)\varphi_{dr3} - \frac{1}{T_r}\varphi_{qr3} \quad (3.35)$$

Where, $\omega_{sl} = \omega_e - \omega_r$

For perfect decoupling control the total rotor flux needs to be aligned with the d-axis so that the q-axis rotor flux is set zero and d-axis rotor flux is maintained constant then equations written as: φ_{qr}=0 ,this implies $\frac{d}{dt}(\varphi_{qr})$=0 and $\varphi_{dr} = \varphi_r$

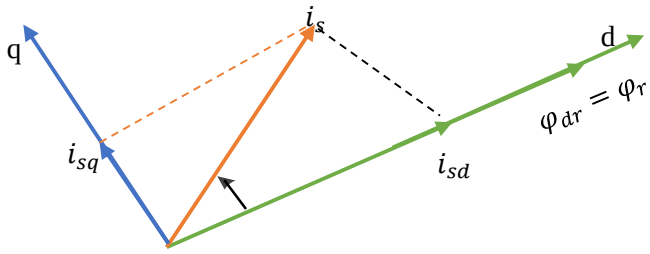

Figure 3.4 Field orientation in d-q reference frame

Substitute into the previous equations to implement the indirect vector control strategy:

$$\theta_e = \theta_{sl} + \theta_r \quad (3.36)$$

$$\varphi_r = L_m i_{ds} \quad (3.37)$$

$$\frac{d}{dt}\varphi_{qr1} - \frac{L_m}{T_r} i_{qs1} + (\omega_e - \omega_r)\varphi_{dr1} + \frac{1}{T_r}\varphi_{qr1} = 0$$

$$\frac{d}{dt}\varphi_{qr3} - \frac{L_m}{T_r} i_{qs3} + 3(\omega_e - \omega_r)\varphi_{dr3} + \frac{1}{T_r}\varphi_{qr3} = 0$$

$$\omega_{sl} = \frac{L_m}{\varphi_r T_r} i_{qs1}$$

The current can be express in terms of flux linkage

$$i_{ds} = \frac{Lr}{LrL_s - Lm^2}\varphi_{ds} - \frac{Lr}{LrL_s - Lm^2}\varphi_{dr} \quad (3.38)$$

$$i_{qs} = \frac{Lr}{LrL_s - Lm^2}\varphi_{qs} - \frac{Lr}{LrL_s - Lm^2}\varphi_{qr} \quad (3.39)$$

$$i_{dr} = \frac{Lr}{LrL_s - Lm^2}\varphi_{dr} - \frac{Lr}{LrL_s - Lm^2}\varphi_{ds} \quad (3.40)$$

$$i_{qr} = \frac{Lr}{LrL_s - Lm^2}\varphi_{qr} - \frac{Lr}{LrL_s - Lm^2}\varphi_{qs} \quad (3.41)$$

To construct the Simulink model of the five phase induction motor, use the following differential equation written in terms of flux linkage:

$$\frac{d}{dt}\varphi_{ds} = v_{ds} - \frac{RsLr}{LrL_s - Lm^2}\varphi_{ds} + \frac{RsLm}{LrL_s - Lm^2}\varphi_{dr} + \omega_e\varphi_{qs} \quad (3.41)$$

$$\frac{d}{dt}\varphi_{qs} = v_{qs} - \frac{RsLr}{LrL_s - Lm^2}\varphi_{qs} + \frac{RsLm}{LrL_s - Lm^2}\varphi_{qr} - \omega_e\varphi_{ds} \quad (3.43)$$

$$\frac{d}{dt}\varphi_{dr} = -\frac{RrLs}{LrL_s - Lm^2}\varphi_{dr} + \frac{RrLm}{LrL_s - Lm^2}\varphi_{ds} + (\omega_e - \omega_r)\varphi_{qr} \quad (3.44)$$

$$\frac{d}{dt}\varphi_{qr} = -\frac{RrLs}{LrL_s - Lm^2}\varphi_{qr} + \frac{RrLm}{LrL_s - Lm^2}\varphi_{qs} - (\omega_e - \omega_r)\varphi_{dr} \quad (3.45)$$

The mechanical equation given by:

$$T_m = T_L + J\frac{d_\omega}{d_t} + B\omega_m \quad \text{where } \omega_m = \omega_r * \frac{2}{P} \quad (3.46)$$

The electromagnetic torque is given by:

$$T_e = T_L + J\frac{d_\omega}{d_t} + B\omega_r \quad \text{where} \quad \omega_r = \omega_m * \frac{P}{2}$$

$$T_{e1} = \frac{5}{2}\frac{P}{2}\frac{L_m}{L_r} i_{qs1}\varphi_{dr1} \quad (3.47)$$

$$T_{e3} = 3\frac{5}{2}\frac{P}{2}\frac{L_m}{L_r} i_{qs3}\varphi_{dr3} \quad (3.48)$$

$$T_e = T_{e1} + T_{e3} \quad (3.49)$$

3.7 Implementation of FOC in Five Phase Induction Motor Drive System

The main aspect of field oriented control method is the coordinate transformation. Basic Field Oriented induction motor drive system is shown in Figure 3.6. The current vector is measured in stationary reference frame α β, where the components of currents is α and isβ must be transformed to the rotating co-ordinate system d-q known as Park transformation. Similarly, the reference stator voltage vector components Vsα and Vsβ must be transformed from the d-q system to α β known as inverse transformation. These transformations require a rotor flux angle 'θ'.

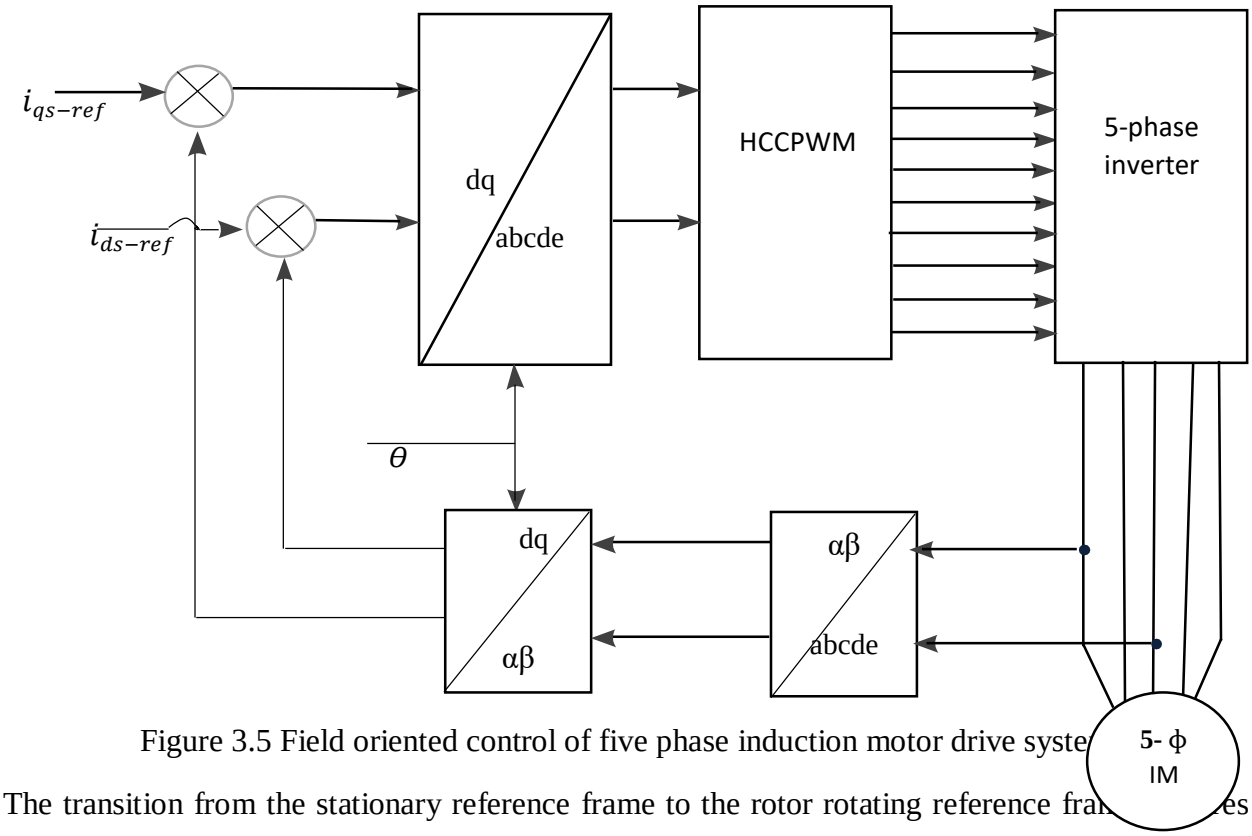

Figure 3.5 Field oriented control of five phase induction motor drive syste

The transition from the stationary reference frame to the rotor rotating reference fra es the determination of position of rotor. The position estimation can be done through sensor-less control. In sensor-less control, an estimator block is needed. Two of the five phase currents are measured because the sum of the five phase currents is equal to zero. This current is fed to the Clarke transformation module, the output obtained from this block is designated as is α and is β. These two components of current act as the input to the Park transformation block, which gives current in the rotating reference frame. Calculation of the two components in the rotating reference frame i_{ds} and i_{qs} is possible by finding the exact rotor flux angular position. These components of

currents are compared with the flux reference current i_{ds-ref} and torque reference current i_{qs-ref}. The portability from asynchronous to synchronous drive can be obtained by simply changing the flux reference and determining the rotor flux position. The torque command i_{qs-ref} is obtained from the speed regulator output. The current i_{qs-ref} obtained from flux relation motor model. It acting as the input to the inverse Park transformation, where the conversion from d-q to α β takes place. The output of this projection gives the component of the stator vector current in the α β stationary reference frame as $i_{\alpha s-ref}$ and $i_{\beta s-ref}$. The rotor flux position is necessary for Park and Inverse Park transformations. Here hysteresis current control modulation techniques are used, that provides advantages such as fastest dynamic response.

3.8 Field Oriented Controller Design

The objective of FOC is to achieve a similar type of controller with an inner torque control loop which makes the motor respond very fast to the torque demands from the outer speed control loop. In field oriented control, the principle of decoupled torque and flux control are applied and it relies on the instantaneous control of stator current space vectors.

Control of induction motor is complicated due to the control of decoupled torque and flux producing components of the stator phase currents. There is no direct access to the rotor quantities such as rotor fluxes and currents. To overcome these difficulties, high performance vector control algorithms are developed which can decouple the stator phase currents by using only the measured stator current, flux and rotor speed.

Speed control of induction motors mainly consist of two loops the inner loop for current and the outer loop for speed. The order of the loops is due to their response; how fast they can be changed. This requires a current loop at least 10 times faster than the speed loop. The design begins with the innermost current loop by drawing the block diagram. But in induction motor system the motor has current controllers which make the current loop. The current control is performed by the comparison of the reference currents with the actual motor currents is done by hysteresis current controller. PI controller has the optimum control dynamics including zero steady state error, fast response (short rise time), no oscillations and higher stability. The necessity of using a derivative gain component in addition to the PI controller is to eliminate the overshoot and the oscillations occurring in the output response of the system.

One of the main advantages of the PI controller is that it can be used with higher order processes including more than single energy storage. The conventional proportional-integral controller remains the most popular design approach used in industrial applications due to its simplicity and reliability for the control of first and second order plants, and even high order plants with well-defined conditions. The gains of the PI controllers can be designed by well-established method. Also, the PI controller is simple to operate and give zero steady state error. But improper selection of gains may affect the system performance making the system unstable. So, proper selection of gains is quite important. Different techniques can be employed for the design of gains of the PI controllers. The method used here is pole- zero cancellation technique. The higher order induction motor drive system is divided into two decoupled subsystems i.e. electrical and mechanical subsystem. The PI controllers are designed for d-q speed controller.

In the pole-zero cancellation technique, the zero of the PI controller is chosen so as to cancel one of the open loop poles of the system.

Here, the ratio of the integral gain to the proportional gain is kept constant and a suitable value of the natural frequency of the first order system is to be chosen.

speed controller design

To achieve linear control, it is necessary to remove the decoupling terms. These terms can be considered as disturbance and are cancelled by using a decoupled method that utilizes nonlinear feedback of the coupling voltage. The transfer function for speed controllers of the vector controlled induction motor drives after removing the decouple term are given as follows

The electromagnetic torque equation of a rotor flux oriented IFOC is given as:

$$T_e = T_L + J\frac{d_\omega}{d_t} + B\omega_r \tag{3.50}$$

$$T_{e1} = \frac{5}{2}\frac{P}{2}\frac{L_m}{L_r} i_{qs}\,\varphi_{dr} \text{ ; let } k_t = \frac{5}{2}\frac{P}{2}\frac{L_m}{L_r}\varphi_{dr} \tag{3.51}$$

Where T_L J, B and ω_r are the load torque ,moment of inertia, coefficient of friction and rotor speed respectively .From equation (3.46) and (3.47) the transfer function of the speed controller plant is given by:

$$G(s)_P = \frac{\omega_r(s)}{i_{qs1}(s)} = \left(\frac{k_t}{Js+B}\right) \tag{3.52}$$

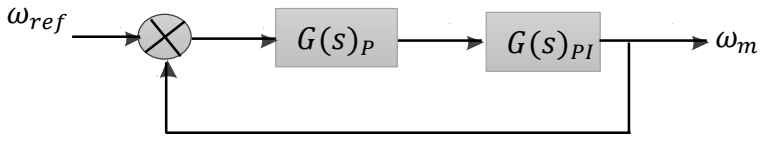

Figure 3.6 closed loop diagram of speed control

T_L , added as the disturbance when design the speed controller.

PI-tuning using symmetric optimization criteria

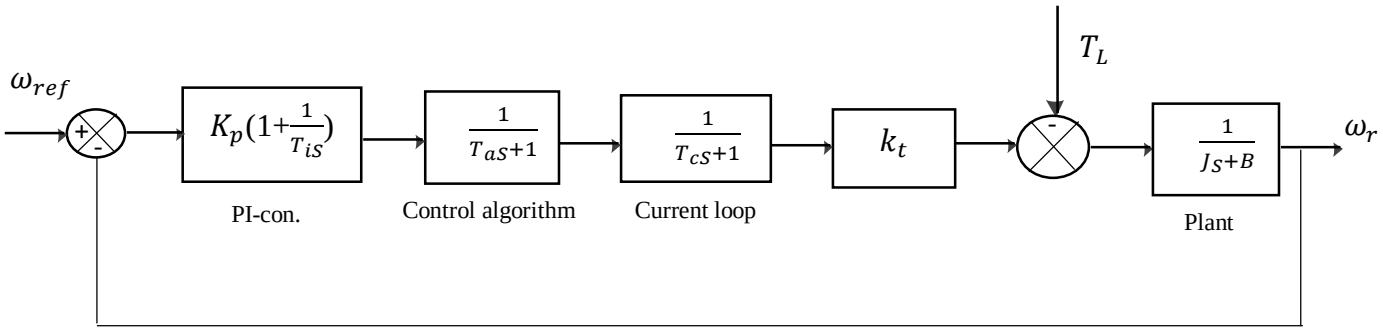

Figure 3.7 PI-speed controller loop

Transfer function of PI $G(s)_C = K_p+\frac{k_p}{s}=K_p(1+\frac{1}{T_{iS}})$

$G_C = K_p(1+\frac{1}{T_{iS}})$ where $T_{iS} =\frac{K_p}{K_i}$ it integral time constant

$$G_P=K_p(1+\frac{1+T_{iS}}{T_{iS}}) \tag{3.53}$$

The control algorithm block represents the time-delay in the form of first order system .The current loop and control algorithm taken as first order transfer function as follow $\frac{1}{T_{cS}+1}$ and $\frac{1}{T_{aS}+1}$

Sampling time taken 0.75msec to find proportional integral gain. The two first order delay transfer function approximated as follow

T_{ac} =2*T_s=0.75*2=1.5msec

From figure 3.7 the open loop and closed loop transfer function as follows:

$$G_{ol}=K_p(1+\frac{1}{T_{iS}}) * \frac{1}{T_{aS}+1} * \frac{1}{T_{cS}+1} * \frac{k_t}{JS+B} \tag{3.54}$$

By approximated the two first order delay transfer function open loop transfer function becomes

$$G_{ol}=K_p(\frac{1+T_{iS}}{T_{iS}})*\frac{1}{T_{ac}+1} *\frac{k_t}{JS+B} \tag{3.55}$$

Closed loop transfer function

$$G_{clo}=\frac{G_{ol}}{1+G_{ol}}=\frac{T_{iS}+1}{\frac{1}{K_tK_P}(T_{iS}(T_{acS}+1)(JS+B))+T_{iS}+1} \quad (3.56)$$

By comparing the closed loop of the system to symmetric optimization transfer function we can determine the gain of PI controller as follows:

$$G_{clso}=\frac{4T_{\mu S}+1}{8T_{\mu}{}^{3}\,S^{3}\,+8T_{\mu}{}^{2}S^{2}\,+4T_{\mu}+1} \quad (3.57)$$

Where T_{μ} the sum of all small delay in loop

$$G_{clo}=\frac{G_{ol}}{1+G_{ol}}=\frac{T_{iS}+1}{\frac{1}{K_tK_P}(T_{iS}(T_{acS}+1)(JS+B))+T_{iS}+1}$$

$$G_{clo}=\frac{T_{iS}+1}{\frac{1}{K_tK_P}(T_iT_{ac}JS^3+T_iJS^2)+T_iS+1} \quad (3.58)$$

Equating symmetric optimization and closed loop transfer function of the system and solve unknown parameters as follows:

$$4T_{\mu}=T_i \quad (3.59)$$

$$8T_{\mu}{}^{3}=\frac{T_iT_{ac}J}{K_tK_P} \quad (3.60)$$

$$8T_{\mu}{}^{2}=\frac{T_iJ}{K_tK_P} \quad (3.61)$$

But $T_i=4T_{\mu}$

By using table 4.1 we can substitute the constants and sampling time we can determine the PI gains.

T_{ac}=1.5msec , J=0.03, K_t=0.815 and we can consider coefficient of friction neglect

Therefore K_tK_P=10, K_P=12.3

$T_i=\frac{K_P}{K_i}$=6msec, T_{μ}=1.5msec, K_i=2044.9

The ζ value is set to 0.707 in this thesis. The value 0.707 generally results in a step response with fast settling time and reasonable overshoot. Increasing the value within the range from 0.707 and 1 will reduce the overshoot of the step response, but will increase the settling time. The design of K_P and K_I is introduce to ensure stability, error tracking and robust operation. The constraint considered in this design is percent of overshoot; settling time and rise time are less than five percent, less than two second and less than two second respectively. The design of K_I and K_P is selected to ensure that all the poles and zeros are located in the left hand side of s-plane and this allows for the required fast and stable response. The location of closed loop transfer function poles

characterizes the control system dynamics. Therefore, the location of the PI controller zero should be on the real axis to make sure that fast dynamics response.

Therefore, $k_i$is taken of 2044.9 and $k_p = 12.3$ .This allows for fast exponentially speed error decaying and acceptable overshoot or undershoots. The location of the PI controller zero k_p/k_i can be designed at any speed. All the poles of the closed loop transfer function lie in the left half of the s-plane then the system has been stable in the operating point.

Design PI Controllers in Discrete System

The transfer function of the PI d-q current controller is written as:

C(s) = $\frac{k_p\left(s+\frac{k_i}{k_p}\right)}{s}$ and the plant equation G_i(s) is given by the equation (3.55).

The design procedure is conducted by calculate the open loop transfer function of the plant, derive the loop gain of the control system using pole zero cancellation method, and lastly obtain the controller parameters from the closed loop transfer function. For real time applications the system is controlled in discrete time domain and therefore the PI controller in Z domain the transfer function $C_z = \frac{k_p(k_p+k_iT)z-k_t}{z-1}$ .The parameter k_p and k_i of the discrete controller are obtained by the following steps [34].

Step-1 calculates the open loop transfer function of the plant. The open loop transfer function of the plant in Z-domain derived as:

$$G_{oiz}= \text{C(z)}[\ G_{zoH}(s)G_i(s)]\text{Z} \tag{3.62}$$

The open loop transfer function becomes:

$$G_{oiz} = (k_p + k_iTs\frac{\text{z}-\frac{k_tK_I}{k_p+K_iT_s}}{z-1}\ )\frac{1}{\sigma L_s y}\left[\frac{1-e^{-yTs}}{z-e^{-yTs}}\right] \tag{3.63}$$

Step-2: deriving the loop gain of the transfer function using pole-zero cancellation method.

From Equation (3.51) using pole-zero cancellation it can be written:

$$\frac{k_p}{k_p+K_iT_s}=e^{-yTs} \tag{3.64}$$

From Equation (3.28) $k_p = K_iT_s\left[\frac{e^{-yTs}}{1-e^{-yTs}}\right]$, then Equation (2.62) becomes:

$$G_{oiz} = k_p + k_iT\frac{1}{\sigma L_s y}\left[\frac{1-e^{-yTs}}{z-1}\right] \tag{3.65}$$

Step-3: determining the controller parameters for a given bandwidth.

$$G_{oiz} = \frac{k_p + k_i T(1-e^{-yTs})}{\sigma L_s y}\left(\frac{1}{z-1+\frac{k_p + k_i T(1-e^{-yTs})}{\sigma L_s y}}\right) \quad (3.66)$$

Equating Equation (3.58) and Equation (3.59)

$$k_p + k_i Ts = \frac{\sigma L_s y\ (1-e^{-B_w Ts})}{1-e^{-yTs}} \quad (3.67)$$

Substitute the value of from Equation (3.28) the proportional and integral gains of d-q current controller gains are obtained as

$$k_i = \frac{\sigma L_s y\ (1-e^{-B_w Ts})}{Ts} \quad \text{and} \quad k_p = \frac{\sigma L_s y\ e^{-yTs}\ (1-e^{-B_w Ts})}{e^{-yTs}}$$

Step-1: Calculate the open loop transfer functions of the plant.

The open loop transfer function of the plant in Z domain can be derived as:

$$G_{owz} = \mathrm{C(z)}[\ G_{zoH}(s) G_i(s) \quad (3.68)$$

Where $G_{zoH}(s) = \frac{1-e^{-Ts}}{s}$ and the numerator $1 - e^{-Ts}$ in the Z domain can be written as:

$1 - z^{-1}$ similarly C(z) can be written as C(z)= $k_p + k_i T \frac{z - \frac{k_p}{k_p + K_i T_s}}{z-1}$ and G_w(s) is also given in in Equation (3.24). Substitute C(z) in to Equation (2.68)

$$\frac{w_r(z)}{\Delta w_r(z)} = \left(k_p + k_i Ts \frac{z - \frac{k_p}{k_p + K_i T_s}}{z-1}\right)\left(\frac{z-1}{z}\, z\, [\frac{G_w(s)}{s}]\right) \quad (3.69)$$

The open loop transfer function becomes:

$$G_{owz} = \left(k_p + k_i Ts \frac{z - \frac{k_p}{k_p + K_i T_s}}{z-1}\right)\left(\frac{1}{f}\,[\frac{1-e^{-xTs}}{z-e^{-xTs}}]\,\frac{1}{k_t}\right) \quad (3.70)$$

Step-2: deriving the loop gain of the transfer function using pole-zero cancellation method.

$$\frac{k_p}{k_p + K_i T_s} = e^{-xTs} \quad (3.71)$$

$$G_{owz} = \left(k_p + k_i Ts\ \right)\left(\frac{1}{f}\,[\frac{1-e^{-xTs}}{z-e^{-xTs}}]\,\frac{1}{k_t}\right) \quad (3.72)$$

Step-3: determining the controller parameters for a given bandwidth.

$$G_{owz} = \frac{k_p + k_i Ts(1-e^{-xTs})}{f}\,\frac{1}{k_t}\left(\frac{1}{z-1+\frac{k_p + k_i T(1-e^{-xTs})}{f}\,\frac{1}{k_t}}\right) \quad (3.73)$$

The proportional and integral gains of speed controller gains are obtained as:

$$k_p + k_i Ts = \frac{f(1-e^{-B_w Ts})}{1-e^{-xTs}}\ k_t$$

$$k_i = \frac{f(1-e^{-B_w Ts})}{Ts}\ k_t \text{ and } k_p = \frac{fe^{-xTs}(1-e^{-B_w Ts})}{1-e^{-xTs}}\ k_t$$

3.9 Fractional order PI Controller for Vector-Controlled Five Phase Induction motor

The mathematical model of induction motor is highly nonlinear [31]. For simplicity, the so-called vector control is commonly applied such that the torque control of induction motors is similar to the control of DC motors. Regarding the scheme of vector-controlled induction motor, the performance of speed control is influenced by the parameter variations and temperature changes. In this paper, based on the vector-controlled scheme, a FOPI speed controller is design to achieve some designated control performance such as disturbance rejection and tracking accuracy. Following some coordinate transformation and decoupling technique, a simplified vector-controlled scheme.

Integer Order PI (IOPI) controller belongs to the dominating form of feedback industrial controllers and there is a continuous effort to improve their quality and robustness. Controlling industrial plants requires satisfaction of wide range of specification. So, wide ranges of techniques are needed. Mostly for industrial applications, integer order controllers are used for controlling purpose. Now day's fractional order (FOPI) controller is used for industrial application to improve the system control performances. The most common form of a fractional order PI controller is the PI^{γ} controller [32]. The orders of integral are not necessarily integer, but any real numbers. As shown in Figure 2.9, The FOPI controller generalizes the conventional integer order PI controller and expands it from point to plane. This expansion could provide much more flexibility in PI control design. The transfer function of such a controller has the following form [33].

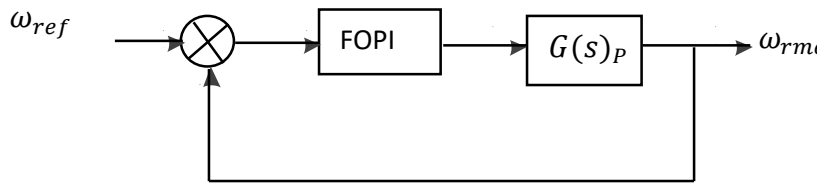

Figure 2.9 Fractional PI controller block diagram

$$G_c(S) = \left(K_{ps} + \frac{K_{is}}{s^{\gamma}}\right) \tag{3.74}$$

From equation (3.49-3.51) and (3.67) the transfer function between the output speed and the speed tracking error is written as:

$$\frac{\omega_{rm}}{\omega_{rm-error}} = \left(K_{ps} + \frac{K_{is}}{s^{\gamma}}\right)\left(\frac{K_t}{J_m s + B_m}\right) \tag{3.75}$$

It is Clear, by selecting λ = 1, a classical PI controller can be recovered. All these classical types of PI controllers are special cases of the PI^{γ} controller.

Advantage of Fractional Order controller

As compared to an integer order controller, a fractional order is supposed to offer the following advantages

i. It is more robust and stable than conventional PI controller.

ii. For systems having large time delays, it provides better results than conventional PI controller.

iii. It provides three different operating conditions as stated above, which is not possible in the case of conventional PI controller.

iv. It can attain improved response for non-minimum phase system.

v. It provides better results for higher order systems as compared to conventional PI controller.

3.9.1 Fractional order PI Controller tuning

The design of PI controller with integer order and Fractional Order dynamics carried out. In the present work Fractional Order PI controllers are tuned based on frequency domain specifications. In this method, a proposed tuning rule is based on a specified desirable behavior of the controlled system related to specified value of the following objectives.

For the tracking purpose, it is desired to have the following requirement:

$$\frac{\omega_{rm}}{\omega_{rm-error}} = 1, \forall \left|G_c G_p K_t\right| \gg 1 \tag{3.76}$$

1. Specified gain crossover frequency

$$\left|C(jw_{cg})G(jw_{cg})\right| = 0dB \tag{3.77}$$

2.Specified phase margin ϕ_m represented as

$$-\pi + \phi_m = \arg((jw_{cg})G(jw_{cg})) \tag{3.78}$$

3.Robustness against variations of gains of the plant, so around the gain cross over frequency phase of the open loop transfer function must be constant

$$(\frac{darg(C(jw_{cg})G(jw_{cg}))}{dw})=0 \text{ at } w=w_{cg} \tag{3.79}$$

4. For rejecting high-frequency noise, at high frequencies the closed loop transfers function must have small magnitude. Thus it is required that at some specified frequency its magnitude be less than some specified gain

$$G(jw) = \frac{C(jw)G(jw)}{1+C(jw)G(jw)} \leq A\ dB\ at\ frequency\ w \geq w_t\ {}^{rad}/_{S} \tag{3.80}$$

5.The sensitivity function must have a small magnitude at low frequencies. To reject output disturbances and tack references it should satisfy the following

$$\left|S(jw) = \frac{1}{1+C(jw)G(jw)} \leq B\ dB\ at\ frequency\ w \leq w_c\ {}^{rad}/_{S}\right| \tag{3.81}$$

The above equation needs to be solved simultaneously, to find out FOPI unknown three parameter P ,I and γ.By solving five design criteria (3.69-3.74) Fractional order PI controller is obtained as.

$$C_{FOPI}(S) = 0.6501 + \frac{0.0542}{S^{1.335}}$$

2.10 Modulation Technique

In order to generate gate pulses for DC current fed five phase current source inverter (CSI) modulation techniques are used. These modulation techniques are also used control the output voltage of the inverter varying the gate pulse to the inverter according to desirable inverter output voltage. These modulation techniques can be either voltage control based or current control based. Voltage control techniques can be divided into three types of Pulse Width Modulation (PWM). First is six steps PWM, second is sinusoidal PWM, and third is SVPWM while current control techniques can be divided into two types HCC and Delta Modulation. The SVPWM and HCC are most commonly used techniques. The HCC is most applied nonlinear control technique due to simple implementation, low software requirement, high reliability, less tracking error and excellent dynamic response.

2.10.1. Hysteresis Current Control(HCC)

Hysteresis current control is implemented by comparing reference current (i*) and actual current (i) and then the actual current wave form is forced to follow the reference current and accordingly the gate pulse is generated and the inverter switches are updated shown in Figure 2.7. This process is applied simultaneously on all the five phases and each five phase reference currents (i_{abcde}*) are compared with actual supply current i_{abcde} to generated the ten gate pulses. Error between two will be pass through comparator with suitable hysteresis band to restrict the current as close as possible to the actual value. The hysteresis band decides the peak to peak current ripple and the switching frequency. Figure 3.10 shows the block diagram for instantaneous current control. As the current exceeded the prescribed hysteresis band value the upper switch turns off and lower switch turns on during fall time. Due to this output voltage falls to lower saturation value from the upper saturation value which results in decay in current. To avoid the shoot through fault at every transition there is provision for lock out time which led to track the actual sinusoidal current waveform within hysteresis band (HB). HB is defined mathematically as:

$$\text{HB}=\text{V}\left(\frac{R_1}{R_1+R_2}\right) \tag{3.82}$$

Where V is comparator biased voltage. Figure 2.10 shows the switching conditions as follows:

If (i*- i) > HB: Upper switch turn on

If (i*- i) < HB: Lower switch turn on

For optimum dynamic performance there must be balance between switching frequency and the current ripples hence for smaller hysteresis band switching frequency is high and lower current ripples.

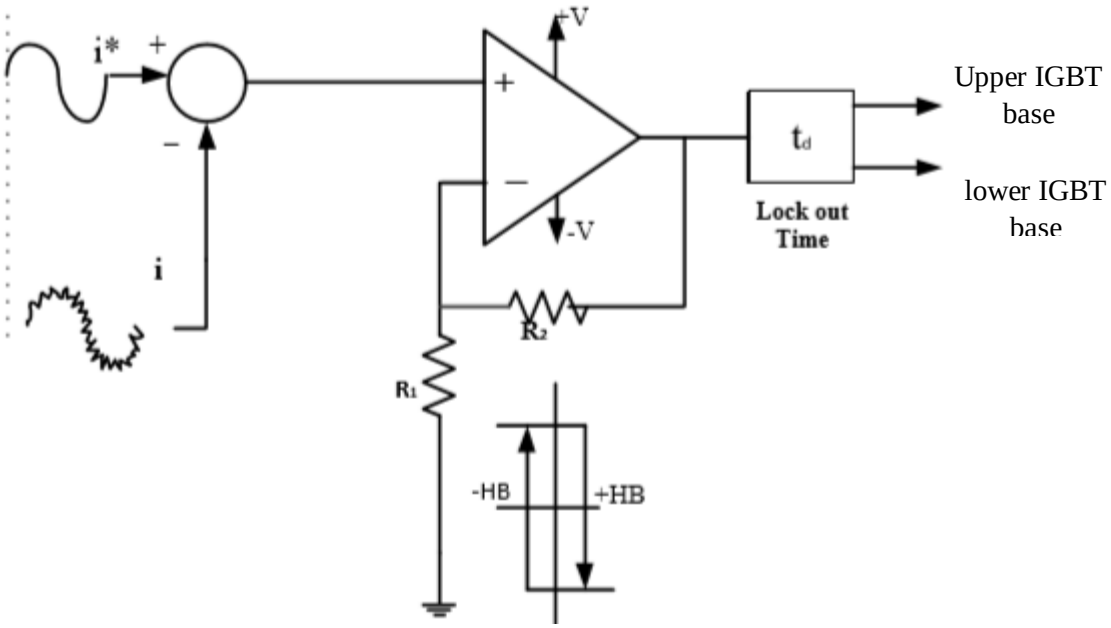

Figure 2.9 Hysteresis current controller

2.10.2 Current Source Inverter

The process of converting DC to AC power is called inversion. Inverter is an electronic device which creates the variable frequency from the fixed DC source in order to drive an induction motor at a variable speed. Depending on the type of DC source supplying the inverter; it can be classified as voltage source inverters (VSI) and current source inverters (CSI). The DC source is usually rectified from the three phase input power. There is a DC link connected between the rectifier and the inverter. A capacitive-output DC link is used for a VSI and an inductive output link is employed in CSI. The circuit diagram for a two-level current source inverter for power applications is shown in figure 2.10

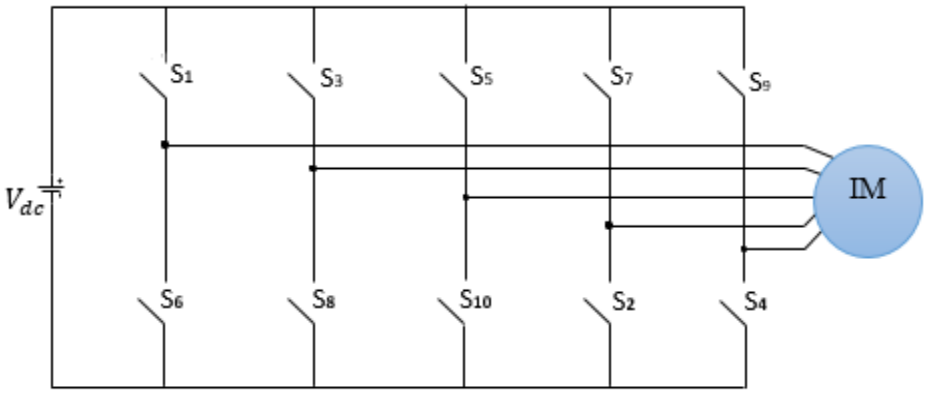

Figure 2.10 Five-phase current source inverter power circuit

A basic five-phase CSI is a ten step bridge inverter, consisting of minimum ten power electronics switches. A step can be defined as the change in firing from one switch to the next switch in proper sequence. For a ten step inverter each step is 36 degree intervals for one cycle of 360 degrees. That means the switches would be gated at regular intervals of 36 degrees in proper sequence to get a five-phase AC output voltage at the output terminal of CSI. The ten switches are divided into two groups; upper five switches as positive group (i.e. S1, S3, S5, S7, S9) and lower five as negative group of switches (i.e. S2, S4, S6, S8, S10). There are two possible conduction modes to the switches such as [27]:

1) 180 degrees' conduction mode and
2) 72 degrees' conduction mode.

In each pattern the gating signals are applied and removed at an interval of 72 degree of the output voltage waveform. By referring to figure 2.11, each switch conducts for 180 degree of a cycle. Switch pair in each arm, i.e. S1-S2; S3-S4; S5-S6; S7-S8 and S9-S10 are turned on with a time interval of 180^0. It means that S1 conducts for 180^0 and S2 for the next 180^0.

In the ten-step 180^0 conduction mode of operation, five switches are on at a time, two from positive group and three from negative group or vice versa, each switch conducts for 180^0 of a cycle. But no two switches of the same leg should be turned on simultaneously in both cases as this condition would short circuit the DC source.

2.10.3. Five-phase 72 Degree Conduction Mode CSI

The power circuit diagram of this inverter is the same as shown in figure 2.10 for the 72^0 mode CSI, each switch conducts for 720 of a cycle. Like 180^0 mode, 72^0mode inverter also require ten steps, each of 360duration for completing one cycle of the output AC voltage.

In the conduction mode 72^0 S1 conducts with S6 for 36^0 then conducts with S8 for another 36^0. S3 will conducts for 72^0 (from 72^0to144^0) 36^0 (from 72^0 to 108^0) with S8 and then conducts another 36^0 (from $108^0$to 144^0) with S10. S5 will conducts 72^0 (from 144^0 to 216^0) with S10 for 36^0 (from $144^0$to 180^0) and then conducts for another 36^0 (from $180^0$to 216^0) with S2. S7 will conducts 72^0 (from $216^0$to 288^0) with S2 for 36^0 (from $216^0$to 252^0) and then conducts for another 36^0 (from 252^0 to 288^0) with S4. S9 will conducts 72^0 (from 288^0 to 360^0) with S4 for 36^0 (from 288^0 to 324^0) and then conducts for another 36^0 (from 324^0 to 360^0) with S6.

Simply, the72^0conduction mode sequence can be written as follows: - S6 S1, S1 S8, S8 S3, S3 S10, S10 S5, S5 S2, S2 S7, S7 S4, S4 S9, S9 S6and S6 S1.

In this conduction mode the chances of short circuit of the DC link voltage source is avoided as each switch conduct for 72^0 in one cycle, so there is an interval of 36^0 in each cycle when no switch is in conduction mode and the output voltage at this time interval is zero [29].

2.10.4. Switching States of the CSI

The operating status of the switches in the current source invertor in figure 2.11 can be represented by switching states. As indicated in Table 2-1, switching state '1' denotes that the upper switch in an inverter leg is on and the inverter terminal voltage V is positive (+Vdc) while '0' indicates that the inverter terminal voltage is zero due to the conduction of the lower switch. There are thirty-two possible combinations of switching states in the CSI. For example, the switching state [10000] corresponds to the conduction of S1, S4, S6, S8 and S10 in the inverter legs A, B, C, D and E, respectively. Among the thirty-two switching states, [11111] and [00000] are zero states and the others are active states

Table 3-1 Definition of Switching State

Switching state	Leg A			Leg B			Leg C			Leg D			Leg E		
	S_1	S_2	V_A	S_3	S_4	V_B	S_5	S_6	V_C	S_7	S_8	V_D	S_9	S_{10}	V_E
1	On	Off	V_{dc}	On	Off	V_{dc}	On	Off	V_{dc}	On	Off	V_{dc}	On	Off	V_{dc}
0	Off	On	0	Off	On	0	Off	On	0	Off	On	0	Off	On	0

Chapter Four

Design of Model Reference Adaptive System

4.1. Introduction

In this chapter, based on the concepts of MRAS, a mathematical model of speed estimation system is presented for sensor-less IFOC Five phase induction motor drive. The model reference approach takes advantage of using two independent machine models, reference model and adjustable model for estimating the same state variable. The estimation error between the outputs of the two computational blocks is used to generate a proper mechanism for adapting the speed. The difference between the two estimated vectors is used to feed a PI controller. The output of the controller is used to tune the adjustable model, which in turn actuates the rotor speed. However, PI controllers may drop the performance level due to the continuous variation in the machine parameters and operating conditions in addition to nonlinearities contributed by the inverter. Based on this, simulation model of sensor-less IFOC five phase induction motor drive using MRAS-PI is developed and validated with extensive simulation results.

4.2 Model Reference Adaptive System

Model Reference Adaptive system (MRAS) is one of the famous speed estimation usually used for sensor-less speed control of induction motor drive. It is one of many promising techniques employed in adaptive control. Among various types of adaptive system configuration, MRAS is important since it leads to relatively easy to implement systems with high speed of adaptation for a wide range of applications. One of the most noted advantage of this type of adaptive system is its high speed of adaptation. This is due to the fact that a measurement of the difference between the outputs of the reference model and adjustable model is obtained directly by the comparison of the states of the reference model with those of the adjustable system.

The block reference model represents demanded dynamics of actual control loop. The block adjustable model has the same structure as the reference one, but with adjustable parameters instead of the unknown ones as shown in Figure 4.1. The MRAS speed estimation structure consists basically of a reference model, adjustable model and an adaptive mechanism.

The error between measured and estimated state variables is then used to drive an adaptation mechanism which generates the estimated speed, for the adjustable model.

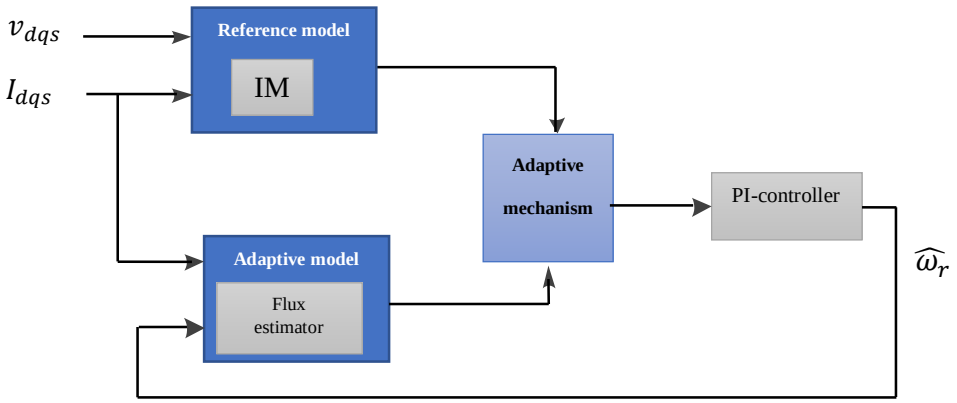

Figure 4.1 General block diagram of rotor flux based MRAS speed estimator

As shown in Figure 3.1, the output of a reference model is compared to the output of an adaptive model until the error between the two models converges to zero. The adaptive model is based on rotor flux estimation and the reference model is the induction motor itself.

4.3 Rotor Flux Based MRAS Speed Estimator Design

MRAS computes a desire state called functional candidate using two different models. In the rotor flux based MRAS, the rotor flux is used as an output value for the model to estimate the rotor speed. The MRAS scheme is based on two independent machine models, the reference model and adaptive model for estimating the same state variable.

In this MRAS scheme the rotor flux linkage (φ_r) is used as speed tuning signal. The motor voltages and currents are measured in a Stationary frame of reference. It is also convenient to express these equations in that stationary frame. The speed can be calculated by the model referencing adaptive system (MRAS), where the output of the reference model is compared with the output of an adjustable model until errors between the two models vanish to zero. A block diagram for speed estimation by this MRAS technique is shown in the Figure 4.2 Consider the voltage model ‘s stator side equations (3.12) and (3.13) which are defined as a reference model.

The model receives the machine stator voltage and current signals and calculates the rotor flux vector signals, as indicated. From the stator voltage equations in the stationary frame, the reference model equations can be obtained as:

Reference Model Equations

$$v_{ds} = R_S\, i_{ds} + \frac{d}{dt}\varphi_{ds} \tag{4.1}$$

$$v_{qs} = R_S\, i_{qs} + \frac{d}{dt}\varphi_{qs} \tag{4.2}$$

$$\varphi_{ds} = L_S\, i_{ds} + L_m\, i_{dr} \tag{4.3}$$

$$\varphi_{dr} = L_r\, i_{dr} + L_m\, i_{ds} \tag{4.4}$$

$$i_{dr} = \frac{\varphi_{dr} - L_m\, i_{ds}}{L_r}$$

$$\varphi_{ds} = L_S\, i_{ds} + \left(\frac{\varphi_{dr} - L_m\, i_{ds}}{L_r}\right)$$

$$\varphi_{ds} = \left(L_s - \frac{{L_m}^2}{L_s\, L_r}\right) i_{ds} + \frac{L_r}{L_m}\varphi_{dr} \tag{4.5}$$

$$\varphi_{qs} = L_S\, i_{qs} + L_m\, i_{qr} \tag{4.6}$$

$$\varphi_{qr} = L_r\, i_{qr} + L_m\, i_{qs} \tag{4.7}$$

$$i_{qr} = \frac{\varphi_{qr} - L_m\, i_{qs}}{L_r} \tag{4.8}$$

$$\varphi_{qs} = \left(L_s - \frac{{L_m}^2}{L_s\, L_r}\right) i_{qs} + \frac{L_r}{L_m}\varphi_{qr} \tag{4.9}$$

Substitute equation (4.5) and (4.9) into equation (4.1) and 4.2) respectively we get reference model of an induction motor in terms of rotor flux as follow:

$$\frac{d}{dt}\varphi_{dr} = \frac{L_r}{L_m} v_{ds} - \frac{L_r}{L_m} R_S\, i_{ds} - \sigma L_S\, \frac{d}{dt} i_{ds} \tag{4.10}$$

$$\frac{d}{dt}\varphi_{dr} = \frac{L_r}{L_m} v_{qs} - \frac{L_r}{L_m} R_S\, i_{qs} - \sigma L_S\, \frac{d}{dt} i_{qs} \tag{4.11}$$

Where φ is flux linkage L_r , L_m , L_S are inductances, R_S is resistance and σ=1$-\frac{{L_m}^2}{L_s\, L_s}$ motor linkage coefficient .

The subscripts r and s denotes the rotor and stator values, respectively, referred to the stator and subscripts d and q denotes d-axis and q-axis components in the stationary reference frame.

The current model flux equations (4.12) and (4.13) are defined as an adaptive model in the Figure 4.2. This model can calculate fluxes form the input stator currents only if the speed signal ω_r is known. With the correct speed signal, ideally, the fluxes calculated from the reference model and those calculated from the adaptive model will match, that is, φ_{dr}= and $\hat{\varphi}_{dr}$ and φ_{qr}=$\hat{\varphi}_{qr}$where $\hat{\varphi}_{dr}$ and $\hat{\varphi}_{qr}$ are the adaptive model outputs.

An adaptation algorithm with P-I control, as indicated, can be used to tune the speed $\hat{\omega}_r$ so that the error $\xi = 0$.

Adaptive model equation

$$\frac{d}{dt}\hat{\varphi}_{dr}=\frac{L_m}{T_r}i_{ds}-\omega_r\hat{\varphi}_{qr}-\frac{1}{T_r}\hat{\varphi}_{dr} \tag{4.12}$$

$$\frac{d}{dt}\hat{\varphi}_{qr}=\frac{L_m}{T_r}i_{qs}-\omega_r\hat{\varphi}_{dr}-\frac{1}{T_r}\hat{\varphi}_{qr} \tag{4.13}$$

Where ω_r rotor electrical speed and $T_r = \frac{L_r}{R_r}$ rotor time constant. The instantaneous angular speed ω_r of the rotor flux vector on an open loop basis can be obtained from the measured voltages and currents. The rotor flux vector angle and its derivative are expressed as:

$$\theta=tan^{-1}\left(\frac{\hat{\varphi}_{qr}}{\hat{\varphi}_{dr}}\right) \tag{4.14}$$

$$\frac{d}{dt}\theta=\frac{\hat{\varphi}_{dr}\left(\frac{d}{dt}\hat{\varphi}_{qr}\right)-\hat{\varphi}_{qr}\left(\frac{d}{dt}\hat{\varphi}_{dr}\right)}{\hat{\varphi}_{dr}^{\,2}+\hat{\varphi}_{qr}^{\,2}} \tag{3.15}$$

Substituting equation (4.12 and 4.13) into (4.15)

$$\frac{d}{dt}\theta=\widehat{\omega_r}+\frac{L_m}{T_r}\left(\frac{\hat{\varphi}_{dr}i_{qs}-\hat{\varphi}_{qr}i_{ds}}{\hat{\varphi}_{dr}^{\,2}+\hat{\varphi}_{qr}^{\,2}}\right) \tag{4.16}$$

The difference between the two estimated vectors is fed to an adaptation mechanism to generate estimated value of rotor speed which is used to tune adaptive model. The adaptation mechanism of conventional rotor flux MRAS is a simple fixed gain linear PI controller. The adaptive scheme for the MRAS estimator can be designed based of Popov's criteria for hyper stability concept [25]. When the rotor flux of the adjustable model is in accordance with that of the reference model of the rotor speed of the adjustable model becomes the real motor speed. The tuning signal e_ω actuate the rotor speed which makes the error signal zero .MRAS of this kind are extensively used to identify plant parameters and inaccessible variables. In designing the adaptation mechanism for a

MRAS. It is important to consider the overall stability of the system and to make sure that the estimated quantity will converge to the desired value with suitable dynamic characteristics. Generally the models are linear time varying systems and ω_r is variable ,but for driving an adaptation mechanism ,treat ω_r as a constant parameter of the reference model. State error equation are obtained by equation (4.12) for adjustable model from the corresponding equations of the of the reference model shown in figure 4.2.

Adaptation Mechanism

It is important to design the adaptation mechanism of MRAS according to the hyper stability concept, which will result in stable and quick response system where the convergence of the estimated value to actual value can be assured with suitable dynamics characteristics [26]. Popov's criterion of hyper stability for a globally asymptotically stable is used in driving the speed estimation relation which represents the difference model and the adjustable model. The parameter ξ should be through a PI block that is found to be satisfactory for adaptive scheme, it gives the below objectives as

$$\xi = (\varphi_{qr}\hat{\varphi}_{dr} - \varphi_{dr}\hat{\varphi}_{qr}) \tag{4.17}$$

Figure 3.2 describes the rotor flux MRAS-PI with both reference and adaptive models for rotor speed estimation. The parameter ξ should be passed through a block that is found to be satisfactory for the adaptive scheme. The speed estimated from MRAS-PI is feedback to speed controller in a sensor-less drive and is compared with reference speed to get the command output.

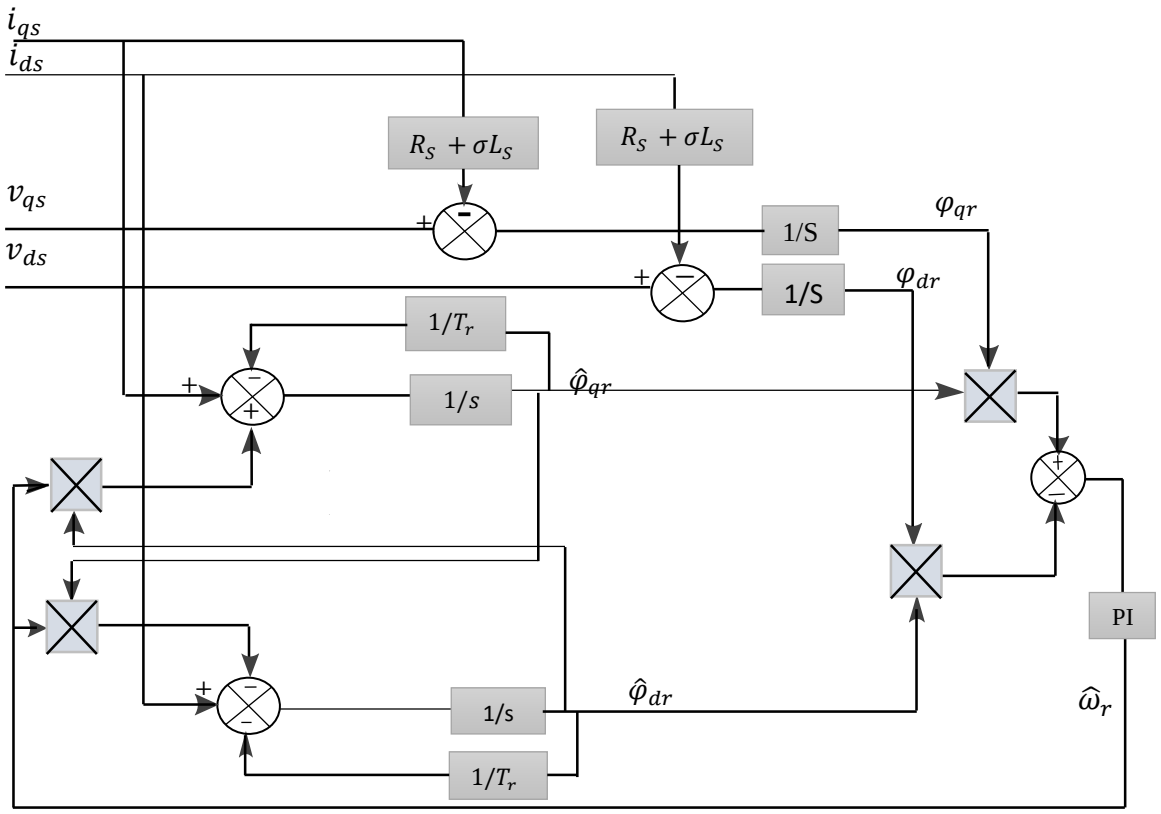

Figure 4.2 Structure of Rotor flux MRAS based Speed estimator

In designing the adaptation algorithm for MRAS, it is important to take account of the overall stability of the system and to ensure that the estimated speed will converge to the desired value with satisfactory dynamic characteristics. We can drive the following relation for speed estimation.

$$\widehat{\omega_r} = \xi\{K_P + \frac{K_I}{S}\} \tag{4.18}$$

where $\xi = (\varphi_{qr}\hat{\varphi}_{dr} - \varphi_{dr}\hat{\varphi}_{qr})$

In steady state $\xi = 0$, balancing the fluxes; in other words, $\varphi_{dr} = \hat{\varphi}_{dr}$ and $\varphi_{qr} = \hat{\varphi}_{qr}$.The MRAS in figure 4.2 can be interpreted as a vector in which the output flux vector from the reference model is reference vector and the adjustable model is a vector phase shifter controlled by $\widehat{\omega_r}$.

4.4 Design of PI for MRAS Based Speed Estimator

In order to drive the PI controller parameter a linearized transfer functions between (ξ) and ($\widehat{\omega_r}$) is obtained. The transfer function obtained from (3.12 &3.13) through linearization with respect to a certain operating point.

$$\hat{\varphi}_{dr} = \frac{-L_r\omega_r\varphi_{qr+L_m i_{ds}R_r}}{R_r + sL_r} \tag{4.19}$$

$$\hat{\varphi}_{qr} = \frac{L_r\omega_r\varphi_{dr+L_m i_{qs}R_r}}{R_r + sL_r} \tag{4.20}$$

Substitute equation (3.19) and (3.20) into equation (3.17)

$$\xi = \frac{L_r\omega_r}{R_r + sL_r}|\varphi_r|^2 \tag{4.21}$$

Let $G_{(s)}$ is $(\frac{\xi_{(s)}}{\omega_r(s)})$ then the simplified closed loop block diagram of rotor flux based MRAS speed estimator is shown in the following diagram.

$$G_{(s)} = \frac{L_r}{R_r + sL_r}|\varphi_r|^2 \tag{4.22}$$

$$\frac{\omega_r}{\widehat{\omega_r}} = \frac{G_{(s)}PIMRAS}{1+G_{(s)}PIMRAS} \tag{4.23}$$

By Comparing the second order characteristic equation of the closed loop transfer function for speed with the standard second order characteristic equation $s^2 + 2\xi w_n s + {w_n}^2$, where w_n is un damped natural frequency and is damping ratio , we can obtain the P-I speed controller gains.

$$K_p = \frac{(2\xi w_n - \frac{1}{T_r})}{|\varphi_r|^2} \tag{4.24}$$

$$K_I = \frac{({w_n}^2)}{|\varphi_r|^2} \tag{4.25}$$

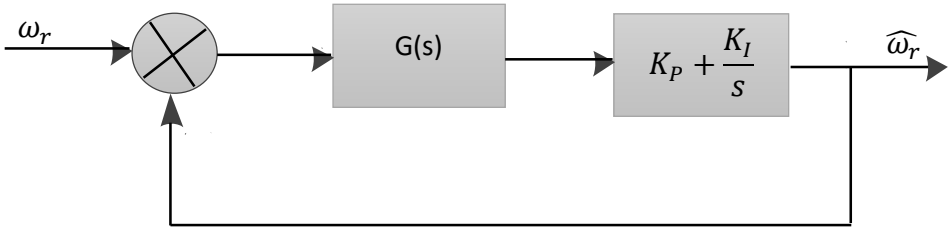

Figure 4.3 Speed estimator dynamics

In (4.23 and 4.24) K_p and K_i are fixed and calculated as a function of rotor flux magnitude φ_r in the steady state which is obtained from current model especially in transients and braking mode .it may cause to significant errors. For the proposed method of work rotor flux magnitude φ_rWhich is calculated from current model is replaced with that of voltage model .

since voltage model have been selected as reference model and current model must follow it .with this replacement the proposed will be in prediction mode .on the other hand K_p and K_i are on-line tuned with respect to instantaneous variation of rotor flux .Instead of its expected value in steady state in this way rotor flux magnitude unexpected variations will be neutralized by on-line tuning of PI parameters and its resulting probable instability will be prevented this modification makes the proposed method adaptive for various conditions. Prediction and adaptations are two characteristics of the proposed method this method does not complicated the algorithm because rotor flux magnitude φ_r is continuously calculated in the MRAS algorithm and thus there is no need for additional computations.

Chapter Five

Simulation Results and Discussion

5.1 Introduction

This chapter presents the simulation of the model and controller of induction motor drive using MATLAB/Simulink software packages. The dynamic performance of the drive for its speed regulation mode is described using pulse width modulation technique. Simulation results are presented and discussed to show the effectiveness of the proposed drive system based on the rotor flux based MRAS speed estimator at different operating conditions such as change in load torque, at different reference speed and speed reversal.

5.2. Simulink Model of the MRAS Based Sensor-less Speed Control of Five Phase Induction Motor

The simulation has been configured based on the proposed model shown in Figure 5.1 to analysis MRAS based sensor-less Speed Control of five phase Induction Motor having parameter mentioned in Table 5.1. In proposed model a five phase squirrel cage induction motor is fed by five phase VSI. The modulation scheme shown for pulse generation to control the output of the inverter. This is a particularly useful add-on to Simulink that provides models for a wide range of power electronics devices and control structures. The Indirect Field Oriented Control (IFOC) as well as the speed estimation structure was implemented using the theory outlined in Chapter 2 and Chapter 4 of this thesis. The induction motor used in this thesis is five phase with rate power of 1.5kw and rated speed 1500 rpm Squarely cage induction motor.

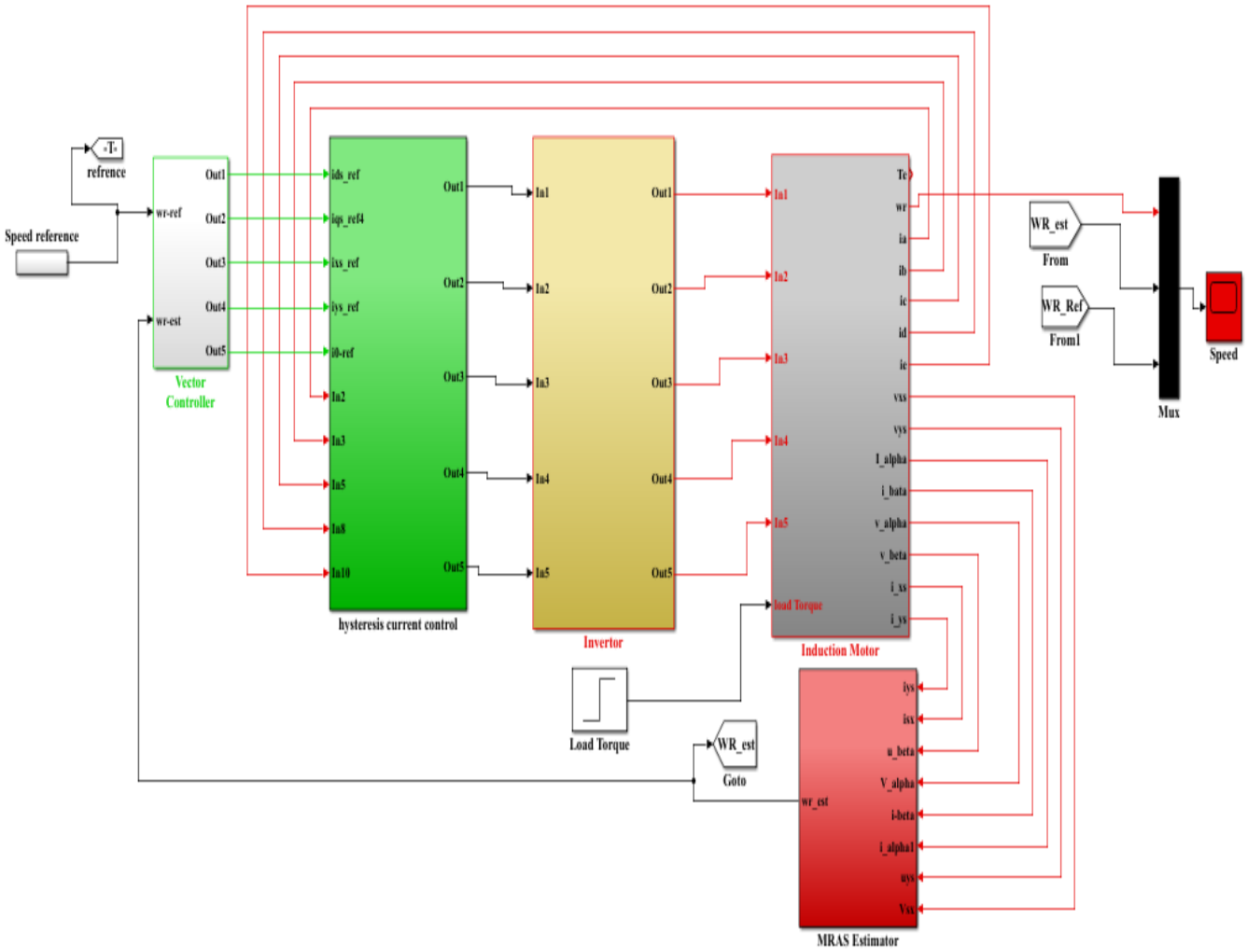

Figure 5.1 Sensor-less Vector Control of five phase IM using rotor flux based MRAS

Coordinate Transformation blocks

The different coordinate transformations such as: Clark transformation, park transformation, Clark-inverse transformation and park-inverse transformation are written in MATLAB source code and embedded in simulation blocks.

Five phase induction motor Simulink model

The simulation model of five-phase IM is not available in the Simulink library. However, it is designed using the stator resistance, rotor resistance, stator inductance, rotor inductance, mutual inductance and moment of inertia as shown in figure 5.1-3. The five phase CSI output voltages are transforming into α-axis voltage and β-axis voltage using the Clark transformation. These voltages also transform in to d-q axis voltages. From these voltages will be determine the actual stator flux and the rotor flux. Then, the d and q axis currents are calculated from d and q axis voltage and flux

variables. After that, the electromagnetic torque is developed from the interaction of stator flux's and stator currents that is taken as actual torque. From the mechanical torque equation and torque load, the rotor speed and rotor position is calculated. And also the overall system block as follow. The parameters of the motor that are used in the simulation are shown in table 5.1.

Table 5-1 Parameters used for simulation

Stator resistance (R_s)	10 Ω
Rotor resistance(R_r)	6.3Ω
Stator inductance (L_s)	0.46H
Rotor inductance(L_r)	046H
Mutual inductance (L_m)	0.42H
Moment of inertia(J)	0.03Kgm^2
Viscus friction(f)	0.003
Number of pole (p)	4
Stator self-inductance(L_{ls})	0.04H
rotor self-inductance(L_{lr}))	0.04H
Rated torque (T)	8.33Nm
Rated phase voltage	220V

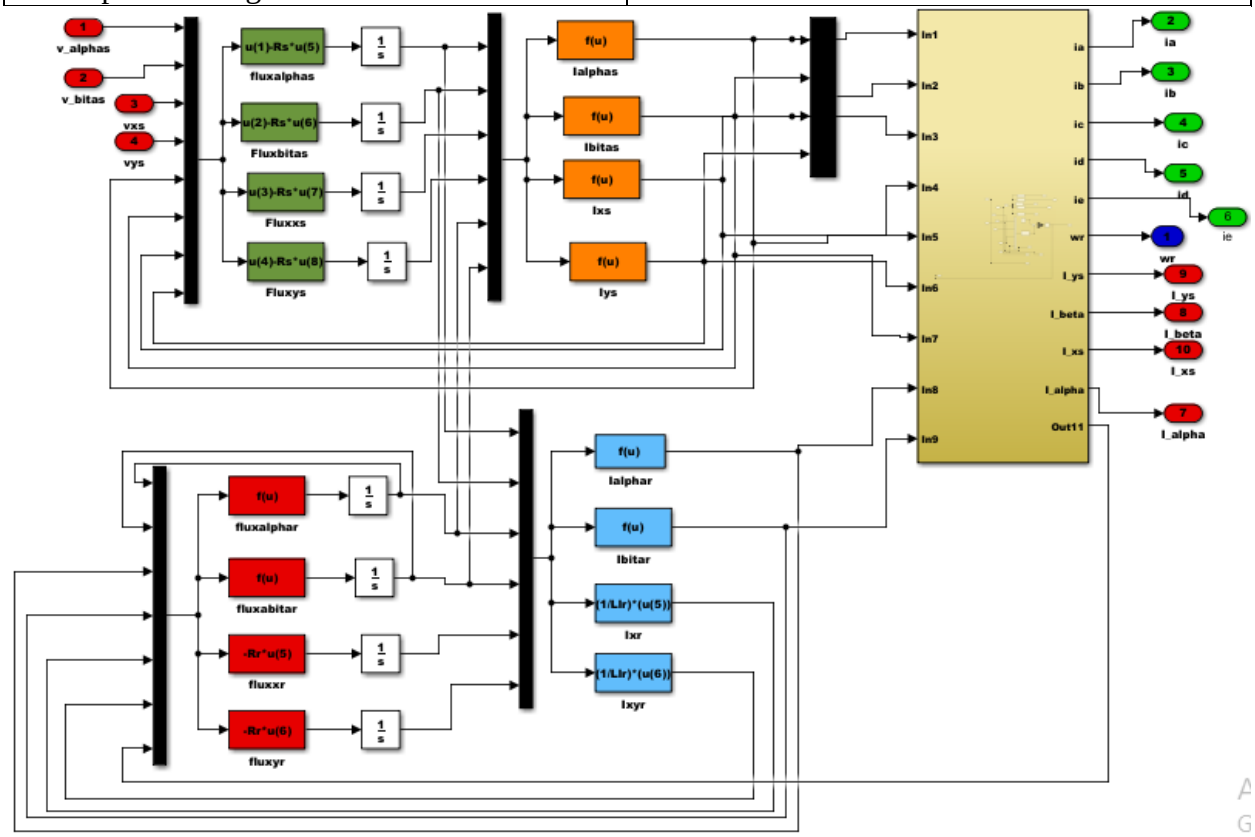

Figure 5.2 Five phase Induction Motor model block diagram

The blocks that had to be constructed were the rotor flux based MRAS speed estimator block seen in Figure 5.3. The rotor flux based MRAS speed estimator calculates the rotor speed used for indirect field oriented control which control hysteresis current control pulse width modulation, this used to drive the current source invertor.

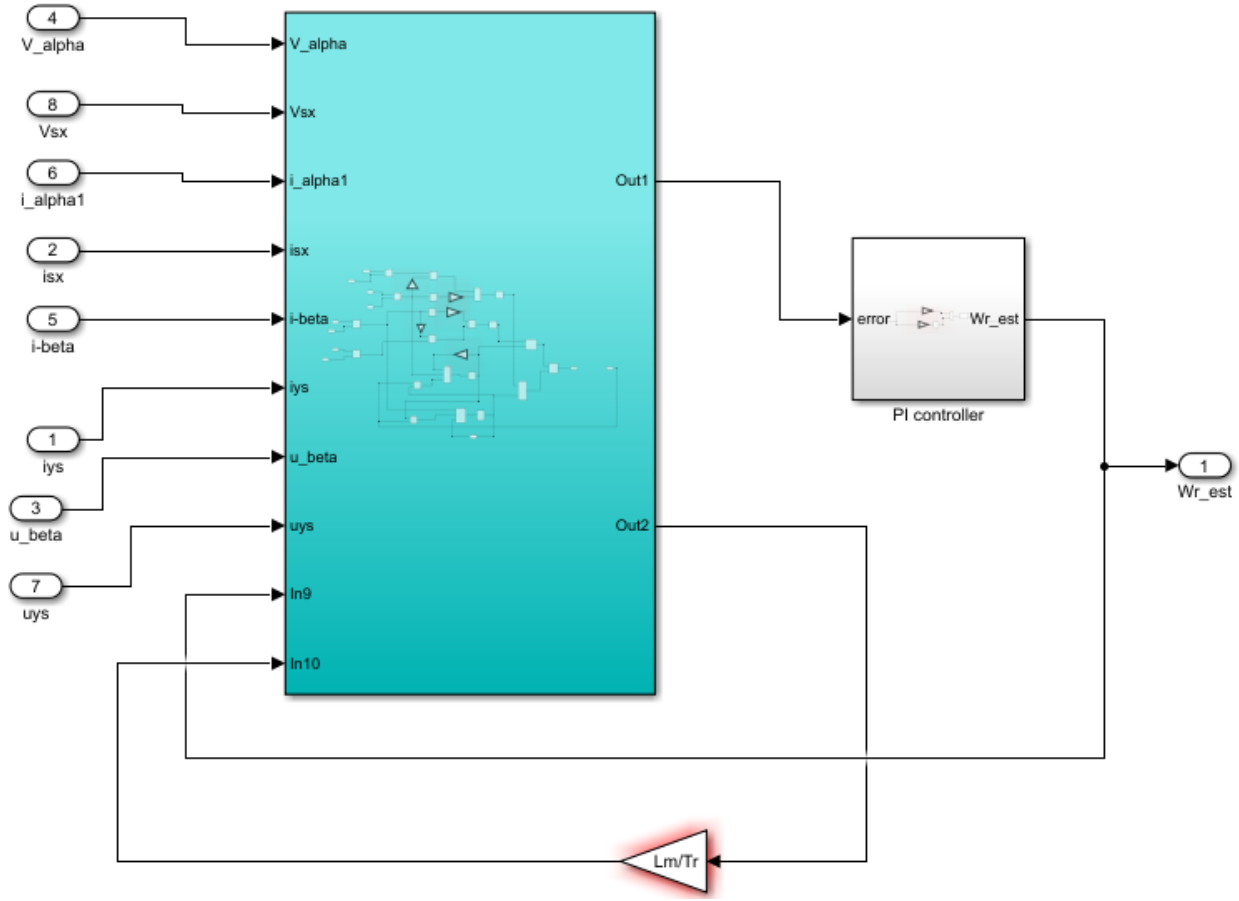

Figure 5.3 Rotor flux based MRAS speed estimator

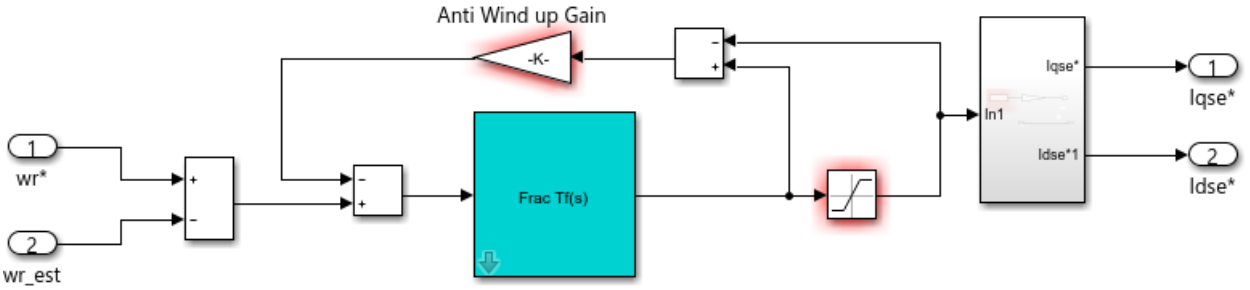

Figure 5.4 FOPI speed controller

5.2.1 Simulation Results

Detailed simulation studies are carried out on MATLAB/ Simulink platform to verify the operating behavior of the proposed scheme. In order to verify the theoretical analysis and the proposed rotor flux based control method, simulations have been carried out using MATLAB software package. The simulation result of MRAS based sensor-less speed control of five phase induction motor drive was carried out to assess its performance. Knowledge of motor's parameter is important for this simulation since the estimator are highly parameter dependent and the effect of the parameter variation was tested based on different condition that are put on their effects on robustness of the speed control. The first simulation result for MRAS based sensor-less speed control of induction motor is the five phase stator current which is generated by the five phase voltage source inverter. This five phase current source inverter is controlled by HCC-PWM blocks for appropriate stator current generation. These five phase phases current should be equal magnitude and 72° phase shift with each other for appropriate rotating flux generation as shown in Figure 5.2.

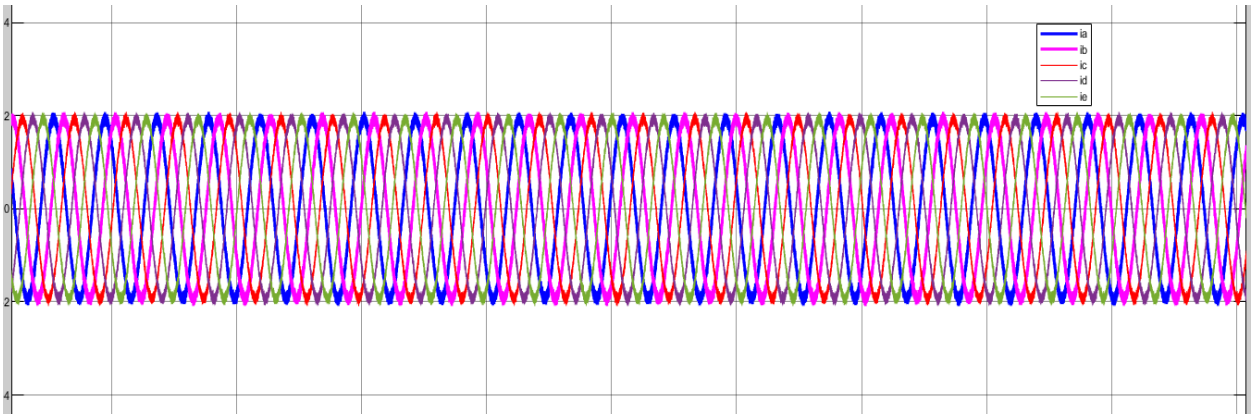

Figure 5.5 Five phase stator current

As it has been seen from the Figure 5.5, the appropriate stator phase current is generated with good accuracy. Hence the system can feed the appropriate stator voltage to the motor. If the voltage applied to the motor is applied with appropriate magnitude and frequency, the speed of the motor is respected as set to the reference value.

A sensor-less IFOC five phase induction motor drive, shown in Figure 5.1, is used where the actual speed feedback signal is replaced by the estimated one. The performance of an estimator assessed based on the ability of the estimated speed to converge to the actual value, especially during transient state. This criterion has been well accepted as a primary indicator when benchmarking the performance of a sensor less speed estimator.

It shows the convergence of the estimated rotor speed to the actual speed. Using the same parameters in the IM and the MRAS estimator, the tracking performance of the estimator can be examined by changing the speed reference of the system. Figure 5.5 and figure 5.6 shows reference, actual, and estimated speed at nominal sinusoidal and step reference input and no load condition.

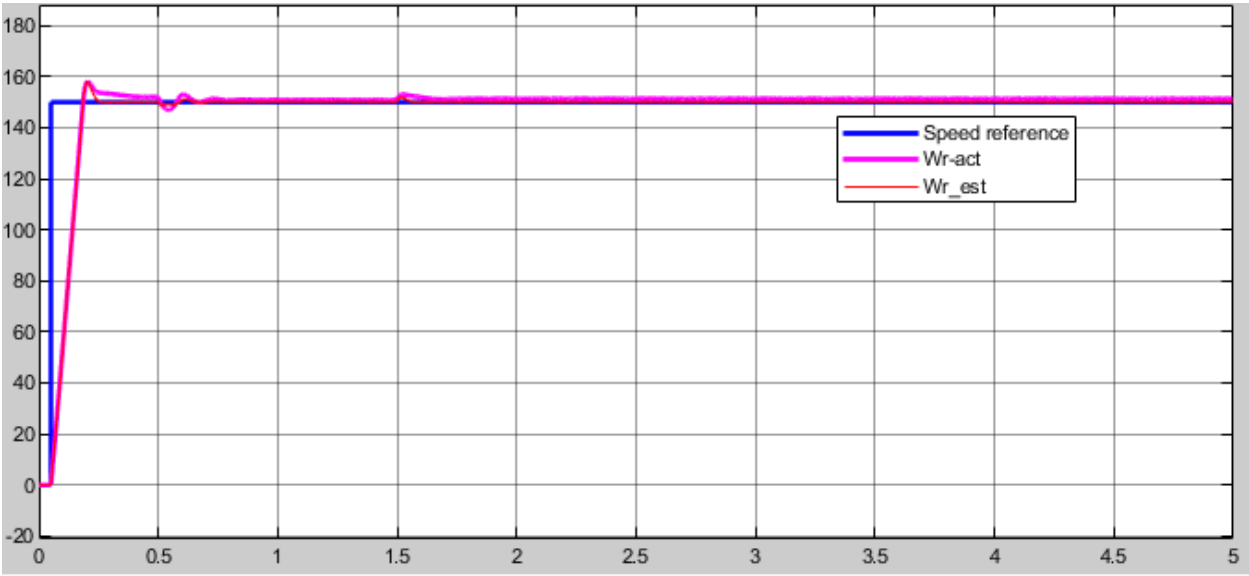

Figure 5.6 The rotor s peed response at 150rad/s step input signal

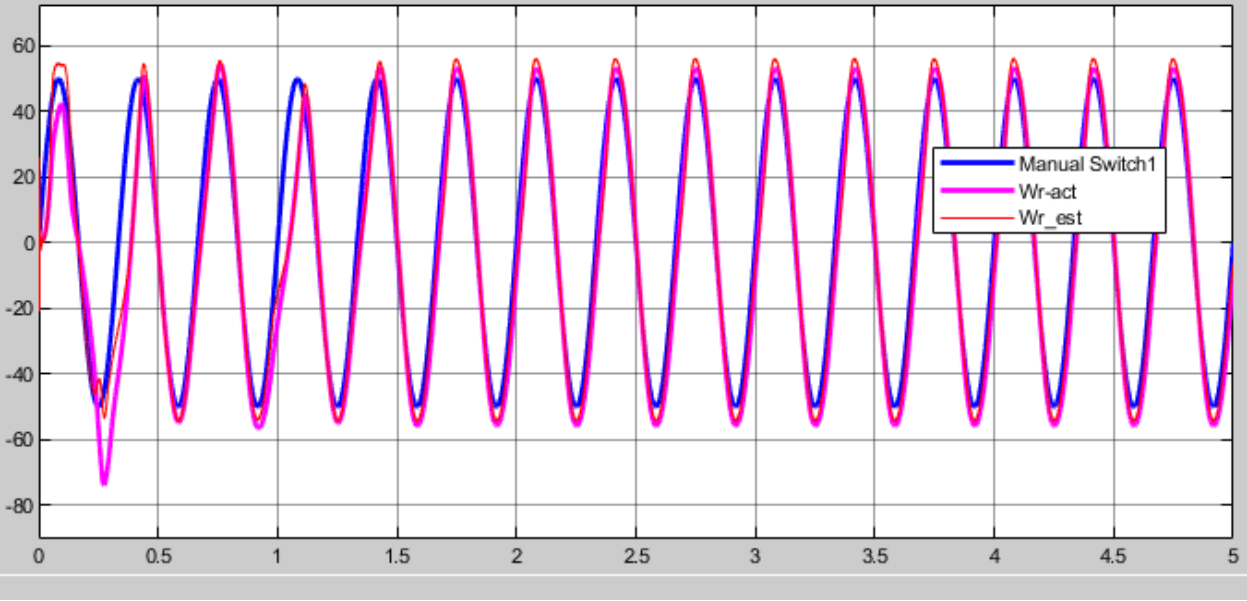

Figure 5.7 The rotor speed response at 50rad/s sinusoidal input signal

We can see in Figure 5.6 and 5.7 that the speed estimation error (error between actual and estimated speed) and tracking speed error (error between reference and estimated speed) are small even at zero speed regions and converge quickly to zero. The aim of this test is to evaluate the performance of the MRAS system at low speed. There is also good field orientation down to zero speed. This means the system is stable at zero speed and continuous operation is possible. There is a short period during settling when the isq response presents some oscillation due to the relatively poor speed estimate (this is large for the full load case). However, after a short period speed and current settle to their respective steady state values.

A reference speed of 10rad/s was initially applied at t = 0.05 seconds, increased to 40rad/s ,70rad/s and 150rad/s at t = 1 second, t=2 second and at t=3.5second respectively. As shown in Figure 4.8 the estimated and the actual speed follow the reference speed with good accuracy and it takes 0.089 second to track the reference speed at different level of speed including low speed region.

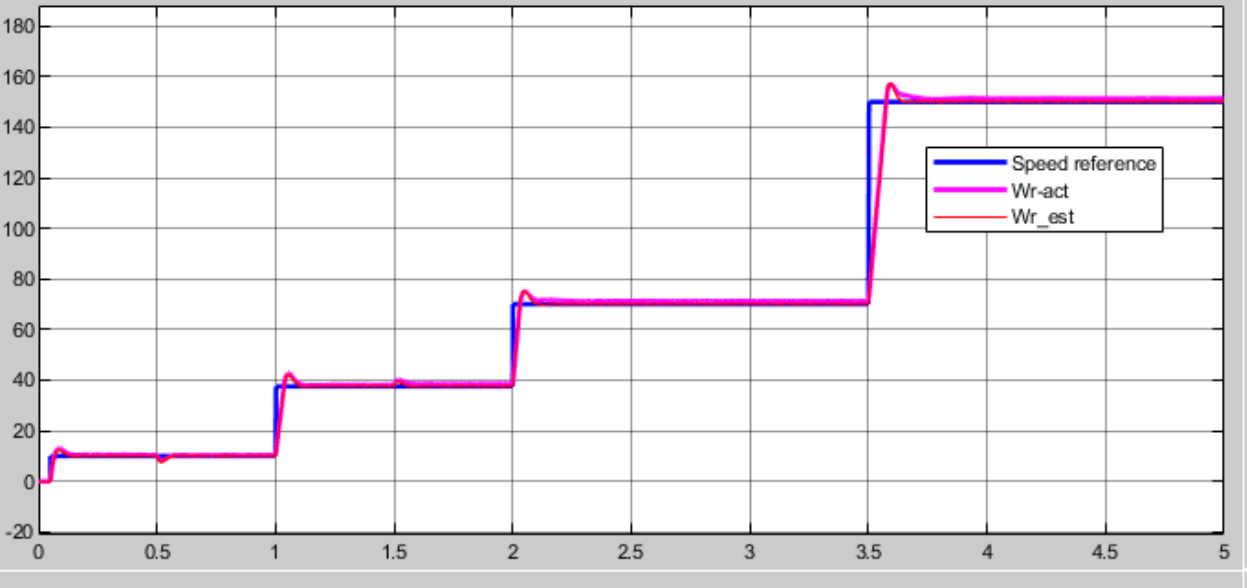

Figure 5.8 Speed response of staircase tracking waveform include low speed region

To test the robustness and torque response quickness toward load torque variation the motor is started with a zero torque and this value is increased at 0.5 seconds 1 seconds,1.5 seconds,3.5 seconds causing a drop in motor speed. This happens because of the mismatch in the torques, i.e.; the developed torque is less than the load torque. To compensate for this mismatch, the controller increases the developed torque by increasing thus in effect the motor speed increases and as we can see, after small variations, the estimation and tracking speed errors converge to zero.

During the simulation shown in figure 5.9, The sensitivity to stator resistance at a nominal speed, the stator resistance was chosen to be equal to 10 Ω and increased and decreased by 50% from its initial value and the other parameters are constant. The three trajectories of estimated, real and reference rotor speed coincide fairly and a very good coincidence is reached. All these results confirm the efficiency of our speed estimation and control.

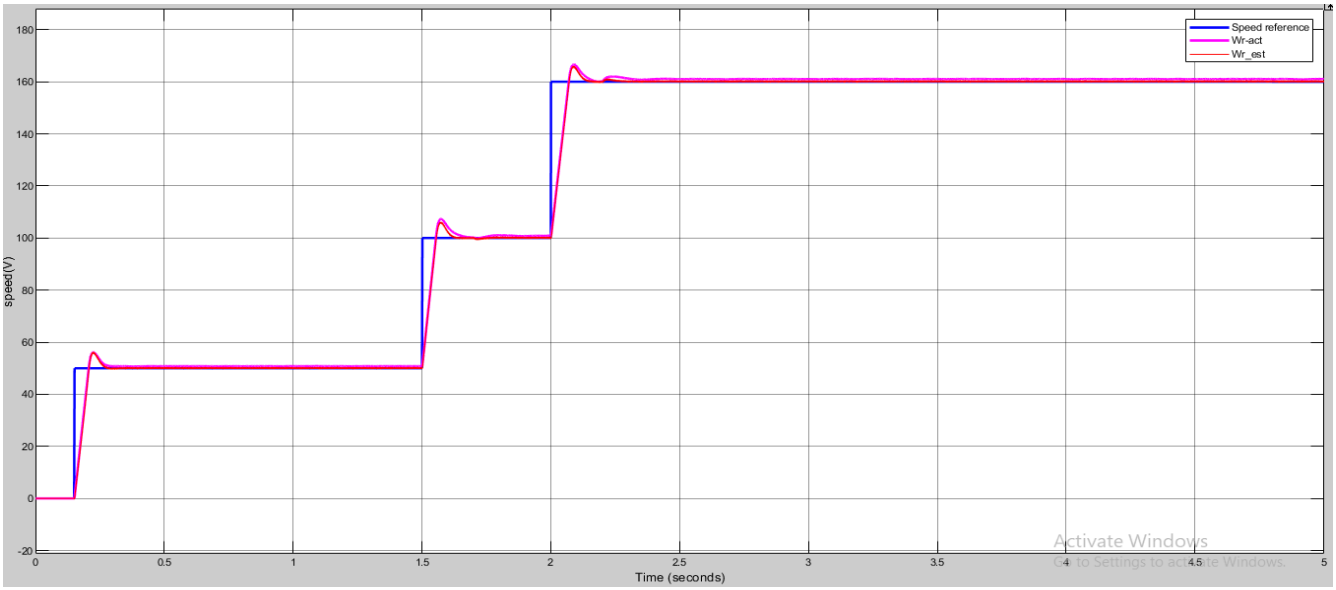

Figure 5.9 50% increasing of Rs from its nominal value for different rotor speed

The load torque is varied in steps motor is no loaded and the load is varied in steps and the corresponding variations in torque, stator current and speed are observed and shown in figure 5.10. It is seen that the stator current increases and speed decreases with increasing load and the motor torque follows the load torque. As can be observed from the simulation result; the simulation model is generated the same output with various parameter of the induction motor.

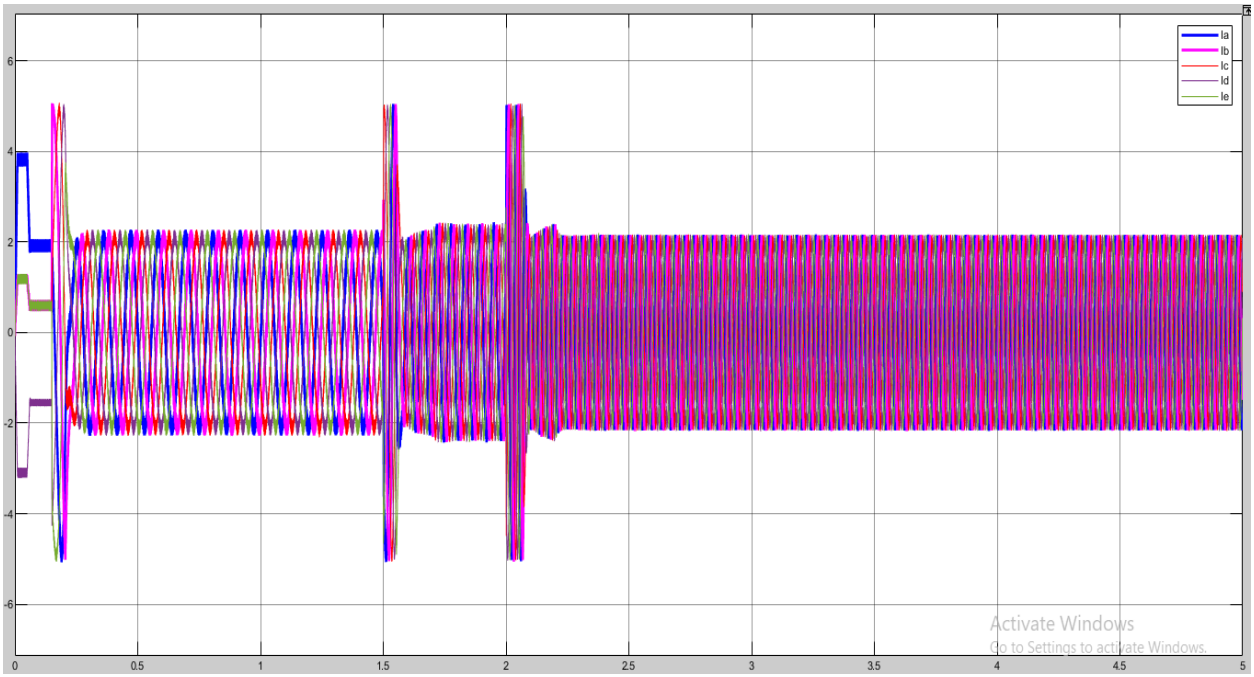

Figure 5.10 Five-phase stator current with different loading conditions

In this case, the induction motor drive is tested under variable speed command with no load and loaded torque. The speed command is 50rad/sec for 1.5 seconds, followed by 160 rad/sec for the next 3.5 seconds. Figure 5.11 shows the speed response of sensor less controlled induction motor drive. it is clear that FOPI controller provided optimum performance in terms of overshoot and settling time. Only rise time remained to be good for conventional PI controller.

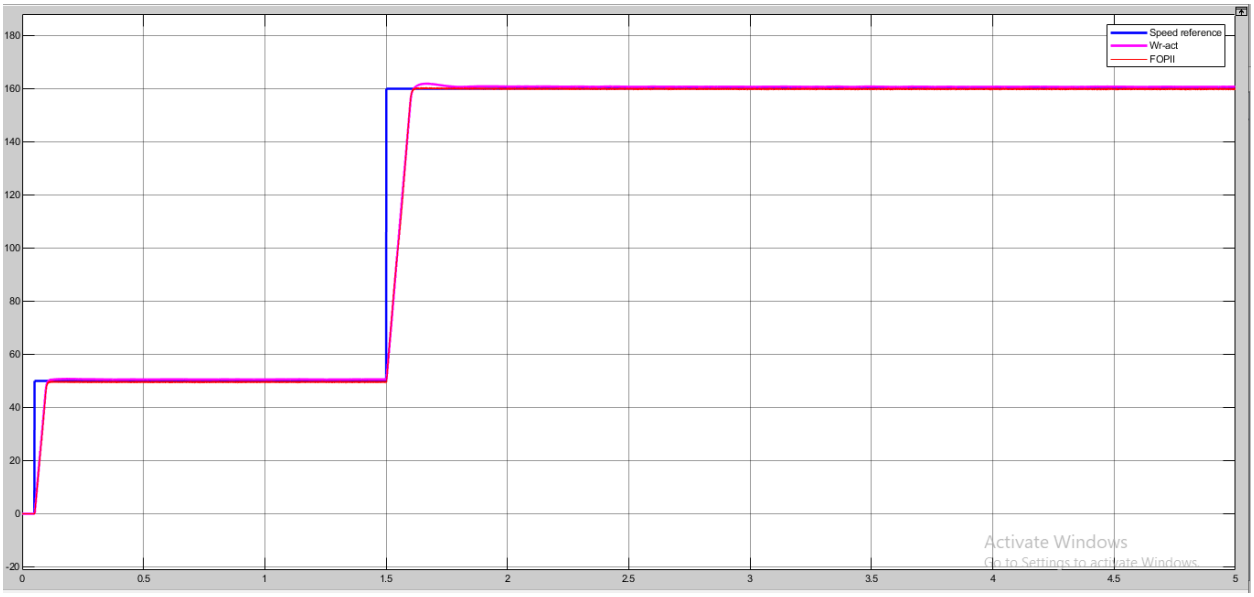

Figure 5.11 Estimated variable speed using FOPI controllers

Chapter Six

Conclusion and Recommendation

6.1 Conclusion

In this thesis, design of MRAS based speed control of sensor-less five phase induction motor using hysteresis current control pulse width modulation (HCC-PWM) technique and performance comparison of FOPI and PI controller has been investigated.

Modeling of five phase induction motor is at first reviewed. The dynamic model of the drive system and its d-q dynamic model in synchronous reference frame with the combined fundamental and third harmonic components have been developed.

The computational techniques used to simplify the rotor flux based MRAS speed estimator design is discussed. Rotor flux based MRAS speed estimator overcome the problem due to mechanical speed sensor and parameter sensitivity for speed control of induction motor has been investigated.

This method is simple and needs a low computation power and has a high speed adaptation. The attainable performance is examined by simulation results for different speed profiles and load condition had shown, that the proposed MRAS estimator was able to estimate accurately the actual speed at low and zero speed.

Simulation results have been presented to compare both the FOPI and conventional PI controllers and it was found that FOPI controller shows better transient performance when compared to conventional PI controller. Also as can be seen from the different speed waveforms the speed error between the reference speed and estimated speed is low when FOPI controller is used in place of conventional PI controller.

These important features are very well shown in the obtained results which indicate that the proposed algorithm shows good speed responses hence it can work with different load torque conditions and with parameters variation.

6.2 Recommendation

Future Research Suggestions is in the following direction.

- For better controlling or to improve system performance and to use in more sensitive application area intelligent controllers such as slide mode controller or fuzzy logic controller are used instead of the ordinary PI controller.
- Performing experimental setup using HVDMCMTRPFC kit with TMS320F28035 control card and analyze the results.

References

[1] Ward E.E., and Harer, H.: "Preliminary investigation of an inverter-fed 5-phase induction motor", Proc. IEE., 1969,116, (6) PP. 980-984.

[2] Namhun Kim and Minhuei Kim, "Modified Direct Torque Control System of Five Phase Induction Motor", Journal of Electrical Engineering & Technology Vol. 4, No. 2, pp. 266271, 2009.

[3] Min-Huei Kim, Nam-Hun Kim, and Won-Sik Baik, "A Five-Phase Induction Motor Speed Control System Excluding Effects of 3rd Current Harmonics Component", Journal of Power Electronics, Vol. 11, No. 3, pp. 294–303 May 2011.

[4] P. Vas, "Sensorless Vector and Direct Torque Control", New York: Oxford Univ. Press, 1998

[5] M. S. Zaky, M Khater, H. Yasin and S. S. Shokralla, "Speed sensorless control of induction motor drives (review paper)", ACTA Electro technical, Vol. 49, No. 3, pp. 221-228, 2008

[6] Blasco Giménez, Ramón High performance sensor-less vector control of induction motor drives. PhD thesis, University of Nottingham's, (1995).

[7] P.L. Jansen and R.D. Lorenz "Transducer less position and velocity estimation in induction a salient ac machines", IEEE Tran. IA, vol. 31, no.2, pp.240-247, Mar/April, 1995

[8] Lu´ıs A. Pereira, S´ergio Haffner, Lu´ıs F. A. Pereira and Ricardo S. da Rosa "Performance Comparison of Five Phase and Three Phase Induction Machines under Steady State including Losses and Saturation" (Rosa (978-1-4799-0223-1/13/$31.00 ©2013 IEEE CEP 90035-190, Porto Alegre, Brazil)

[9] Martin Jones, Emil Levi, Slobodan N. Vukosavic "Independent Control of Two Five-Phase Induction Machines Connected in Parallel to a Single Inverter Supply" International Journal of Engineering, Science and Technology Vol. 2, No. 2, 2010, pp. 136-154

[10] A. Iqbal and E. Levi, "Space Vector Modulation Schemes for a Five-Phase Voltage Source Inverter," European Conference on Power Electronics and Application. 2005

[11] Tze-Fun Chan and Keli Shi, "Applied intelligent control of induction motor," Singapore: Wiley 2011.

[12] Mario J. Duran, Francisco Salas and Manuel R. Arahal, "Bifurcation Analysis of Five Phase Induction Motor Drives with Third Harmonic Injection", IEEE Transactions on industrial electronics, vol. 55, no. 5, May 2008.

[14] H. Xu, H. A. Toliyat, and L. J. Petersen, "Five-phase induction motor drives with DSP based control system," IEEE Transactions on Power Electronics, vol. 17, No. 4, pp. 524533, July 2002.

[15] C. Schaulder, "adaptive speed identification for vector control of induction motors without rotational transducer" IEEE Transaction on industry applications vol.28, no.5, pp.1054-1061,1992

[16] R. Di Gabriele, F. Parasiliti, M. Tursini, Digital Field Oriented Control for Induction Motors: implementation and experimental results Universities Power Engineering Conference (UPEC97)

[17] Bimal K. Bose, "Modern Power Electronics and AC Drives", Condra Chair of Excellence in Power Electronics, The University of Tennesse Knoxville.

[18] Huangsheng Xu, Hamid A. Toliya and Lynn J. Petersen, "Rotor Field Oriented Control of Five-Phase Induction Motor with the Combined Fundamental and Third Harmonic Currents", IEEE, 2001.

[19] Min-Huei Kim, Nam-Hun Kim, and Won-Sik Baik, "A Five-Phase Induction Motor Speed Control System Excluding Effects of 3rd Current Harmonics Component", Journal of Power Electronics, Vol. 11, No. 3, pp. 294–303 May 2011.

[20] F. Blashke, "The principle of field orientation as applied to the new trans vector closed loop control system for rotating field machines," siemens Review, vol.34, PP.217220 May 1972.

[21] Mircea Popescu, "Induction Motor Modeling for Vector Control Purposes", Helsinki University of Technology Department of Electrical and Communications Engineering Laboratory of Electro mechanics, 2000.

[22] Bimal K. Bose, "Modern Power Electronics and AC Drives."; The University of Tennesse. Knoxville

[23] L. Umanand and S. Bhat, "Online estimation of stator resistance of an induction motor for speed control applications," IEE Proc. Electr. Power Appl., vol. 142, pp. 97– 103, Mar. 1995.

[24] P. Zhang, Bin Lu, and T.G. Habetler; "A Remote and Sensorless Stator Winding Resistance Estimation Method for Thermal Protection of Soft-Starter-Connected Induction Machines", IEEE Transactions on Industrial Electronics, Vol. 55, No. 10, Pp. 3611-3618, October 2008

[25] G. Sneha Sai, Ch. Rajya Lakshmi, Ch. Vishnu Chakravarthi, "Speed Estimation of Sensorless Induction Motor through Vector Control Using MRAS and Direct Synthesis Test", International Journal for Modern Trends in Science and Technology, Vol. 02, Issue 11, 2016, pp. 116-123.

[26] G. K. Nisha, Z. V. Lakaparampil and S. Ushakumari, "FFT Analysis for Field Oriented Control of SPWM and SVPWM Inverter fed Induction Machine with and Without Sensor",

International conference on Advance Engineering Technology(ICAET'13), Mysore, India, pp. 34-43, 27 January 2013.
[28] A. Almula and G.M. Gebreel, "Simulation and Implementation of Two level and Three Level Inverters by MATLAB and Rt-Lab", master's thesis, 2011.
[29] N. Patra, "Study of Induction Motor Drive with Direct Torque Control Scheme and Indirect Field Oriented Control Scheme Using Space Vector Modulation", master's thesis, June 2013.
[30] Hace, A., Jezernik, K., Sabanovic, A., SMC with disturbance observer for a linear belt drive, IEEE ISIE 2005, June 20-23, Dubrovnik, Croatia.
[31] D.W. Novotny and T. A. Lipo, Vector Control and Dynamics of AC Drives, Great Britain: Oxford University Press, 1996
[32] I. Podlubny "Fractional-order systems and controllers", IEEE Transactions on Automatic Control, 1999, 44(1):208–214.
[33] Arijit Biswas, Swagatam Das, Ajith Abraham and Sambarta Dasgupta, "Design of fractional-order controllers with an improved differential evolution", Engineering Applications of Artificial Intelligence, Volume 22, Issue 2, pp. 343-350, March 2009.
[34] workagegn Tatek "model reference adaptive based speed control of induction motor" International Journal of Scientific & Engineering Research Volume 8, Issue 6, June-2017 ISSN 2229-5518